JGS
Journal of the Geological Society

Research article

Published online October 4, 2018 https://doi.org/10.1144/jgs2018-090 | Vol. 176 | 2019 | pp. 78–96

Tectonic motion in oblique subduction forearcs: insights from the revisited Middle and Upper Pleistocene deposits of Rhodes, Greece

Jean-Jacques Cornée[1,2*], Frédéric Quillévéré[3], Pierre Moissette[4,5], Jan Fietzke[6], Gatsby Emperatriz López-Otálvaro[2,3], Mihaela Melinte-Dobrinescu[7], Mélody Philippon[1], Douwe J.J. van Hinsbergen[8], Konstantina Agiadi[4], Efterpi Koskeridou[4] & Philippe Münch[2]

[1] Géosciences Montpellier, Université de Montpellier, Université des Antilles, CNRS, Pointe à Pitre, Guadeloupe, FWI, France
[2] Géosciences Montpellier, Université de Montpellier, Université des Antilles, CNRS, Montpellier, France
[3] Université Lyon, Université Lyon 1, ENS de Lyon, CNRS UMR 5276 LGL-TPE, F-69622 Villeurbanne, France
[4] National & Kapodistrian University of Athens, Faculty of Geology and Geoenvironment, Department of Historical Geology & Palaeontology, 15784, Athens, Greece
[5] Muséum National d'Histoire Naturelle, Département Histoire de la Terre, 8 rue Buffon, 75005 Paris, France
[6] GEOMAR, Helmholtz Centre for Ocean Research Kiel, Wischhofstrasse 1-3, 24148 Kiel, Germany
[7] National Institute of Marine Geology and Geoecology, 23–25 Dimitrie Onciul Street, PO Box 34–51, 70318 Bucharest, Romania
[8] Department of Earth Sciences, Utrecht University, Princetonlaan 8A, 3584 CB Utrecht, the Netherlands
J.-J.C., 0000-0003-0542-098X; J.F., 0000-0002-5530-7208; G.E.L.-O., 0000-0001-6808-8123; M.P., 0000-0002-0823-8545; K.A., 0000-0001-8073-559X
* Correspondence: jean-jacques.cornee@gm.univ-montp2.fr

Abstract: **Abstract:** The sedimentary model of coastal deposits in eastern Rhodes over the last 2 Ma is refined and improved in accuracy. New field investigations and U/Th dating of *Spondylus* bivalve shells, combined with micropalaeontological and sedimentological data, allow the recognition of four synthems separated by major erosional surfaces. We present here evidence for two of these erosional surfaces. This new model allows the identification and quantification of the vertical movements recorded by the studied exposures. The history of these vertical motions is characterized by two periods of uplift and two periods of subsidence. Such an evolution is unique at the regional scale in the eastern Hellenic forearc. We interpret these results as reflecting the individualization of Rhodes as a single tectonic block during increasing trench bending. This trench bending is accommodated by an increase in the curvature of the forearc during the last 2 Ma.

Supplementary material: U/Th dating on spondylid shells, index calcareous nannofossils and Khallithea and Faliraki Road sections are available at https://doi.org/10.6084/m9.figshare.c.4211357

Received 1 May 2018; **revised** 17 August 2018; **accepted** 24 August 2018

For the last 40 years, the sedimentary record has been used to reconstruct the vertical movements of the Earth's surface, i.e. subsidence and uplift, in a variety of geodynamic settings, allowing researchers to visualize the strain pattern at plate boundaries and leading to a better understanding of the large-scale mechanical behaviour of the lithosphere (e.g. McKenzie 1978; Vergés *et al.* 1998; Carminati *et al.* 1999; van der Meulen *et al.* 1999; Mackay *et al.* 2005; Cloething *et al.* 2006; Cloething & Burov 2011). More specifically, the strain pattern in the upper plate in a subduction zone directly reflects the dynamics of the down-going slab, i.e. trench bending, variations in dip and velocity, and heterogeneous buoyancies (e.g. Shemenda 1994; Lallemand 1999; von Huene & Ranero 2003; Clift & Vannucchi 2004; Schlaphorst *et al.* 2016; Saillard *et al.* 2017). Constraining the amount and timing of vertical motion of tectonic origin affecting the overriding plate in such geodynamic settings is of great interest and can be achieved via a detailed investigation (logging and dating) of the sedimentary record. Most subduction zones show a curved trench, reflecting progressive trench bending during their evolution. Trench bending can result from the subduction of a buoyant anomaly (e.g. the Andes; Isacks 1988) or extrusion of the upper plate combined with trench rollback, which triggers extension along the trench (e.g. the Mariana, Scotia, Lesser Antilles and Hellenide arcs; Wallace *et al.* 2005, 2008). The bending of the trench causes oblique subduction, which, in turn, triggers strain partitioning within the upper plate (Katili 1970; McCaffrey 2009).

We investigated the eastern region of the Hellenic forearc, which is characterized by relatively rapid trench bending attributed to combined trench rollback, extrusion of the upper plate to the SW and oblique subduction (e.g. Angelier *et al.* 1982; Meulenkamp *et al.* 1994; Gautier *et al.* 1999; Wallace *et al.* 2005, 2008; van Hinsbergen & Schmid 2012; Philippon *et al.* 2014). The Hellenic subduction zone is characterized by a slab of African lithosphere *sensu lato*, which subducts below the Eurasian plate. The post-45 Ma evolution of this region has been peculiar because this slab carried two buoyant microcontinents. These microcontinents entered the subduction zone and locked it, resulting in the formation of two suture zones (the Vardar and Pindos suture zones) and triggering southward slab rollback and associated migration of the volcanic arc (van Hinsbergen *et al.* 2005*a*; Brun & Faccenna 2008; Jolivet & Brun 2010; Jolivet *et al.* 2013). The trench progressively bent during this southward rollback event to reach its present day curvature. This trench bending, combined with rollback, resulted in an increasing obliquity of the subduction zone over time, which has been accommodated by strain partitioning within the upper Eurasian plate (Philippon *et al.* 2014; Brun *et al.* 2016).

To quantify and identify this strain partitioning, we used the palaeobathymetry corrected from the palaeosea-level to provide rough estimations of the vertical motion recorded by the island of Rhodes and compared this vertical motion with that of other islands along the eastern part of the Hellenic trench. We established a new scheme for the upper Pleistocene deposits of Rhodes, including previously published data. This scheme allows a reassessment of the vertical motion in this part of the Hellenic forearc and allows us to refine the timing of the rotation of the vertical axis since 2 Ma.

Geological setting

The Hellenic forearc (Fig. 1a) has been formed by the subduction of the African plate beneath Eurasia since the Cretaceous (Jolivet *et al.* 2013). It consists of a deformed stack of upper crustal nappes and ophiolites accreted on long-lived subduction continental and oceanic crust (Bonneau 1984; van Hinsbergen *et al.* 2005*b*) and overlain unconformably by late Neogene to Recent deposits (Mutti *et al.* 1970). This nappe stack originally trended WNW–ESE overall, curving only slightly around the stable Eurasian margin. However, since Eocene, and particularly Middle Miocene time, the Aegean forearc became strongly curved due to opposite rotations, clockwise in the west and counterclockwise in the east (Morris & Robertson 1993), which were accommodated by major arc-normal and arc-parallel extension in the back-arc and forearc Aegean region (Gautier *et al.* 1999; van Hinsbergen & Schmid 2012; Philippon *et al.* 2014). This increased curvature has led, since the Pliocene, to stretching along the eastern part of the forearc. This stretching is accommodated along NE–SW-trending strike-slip faults parallel to the plate boundary with Africa (e.g. ten Veen 2004; Tur *et al.* 2015; Kaymakcı *et al.* 2018) and involves anticlockwise rotation and multiple tilting (Fig. 1b). The opening of the 4000 m deep Rhodes Basin, east of the island of Rhodes, is a noticeable event attributed to a transtensional horsetail splay of the oblique Africa–Aegean plate boundary (Woodside *et al.* 2000; Hall *et al.* 2009). The opening of this basin was originally thought to have started in the Pliocene because Messinian evaporites were not observed (Woodside *et al.* 2000). However, the recent finding of a thin layer of such evaporites (Aksu *et al.* 2018) shows that the basin had already started opening before 6 Ma. The opening of this basin promoted considerable sinking and then uplift events on Rhodes, which resulted in the deposition of the Pleistocene marine sediments that crop out on the island today.

The marine Pleistocene deposits of Rhodes crop out on the eastern coast and patchily on the northern coast (Figs 2 & 3). Their stratigraphy, sedimentology and palaeontological content have been studied by many researchers, including Keraudren (1970), Mutti *et al.* (1970), Meulenkamp *et al.* (1972), Broekman (1974), Løvlie *et al.* (1989), Frydas (1994), Hanken *et al.* (1996), Hansen (1999), Kovacs & Spjeldnaes (1999), Nelson *et al.* (2001), Thomsen *et al.* (2001), Rasmussen *et al.* (2005), Nielsen *et al.* (2006), Cornée *et al.* (2006*a*; 2006*b*), van Hinsbergen *et al.* (2007), Joannin *et al.* (2007), Thomsen *et al.* (2009), Titschack *et al.* (2013) and Moissette *et al.* (2013, 2016). Following the pioneering work of Hanken *et al.*

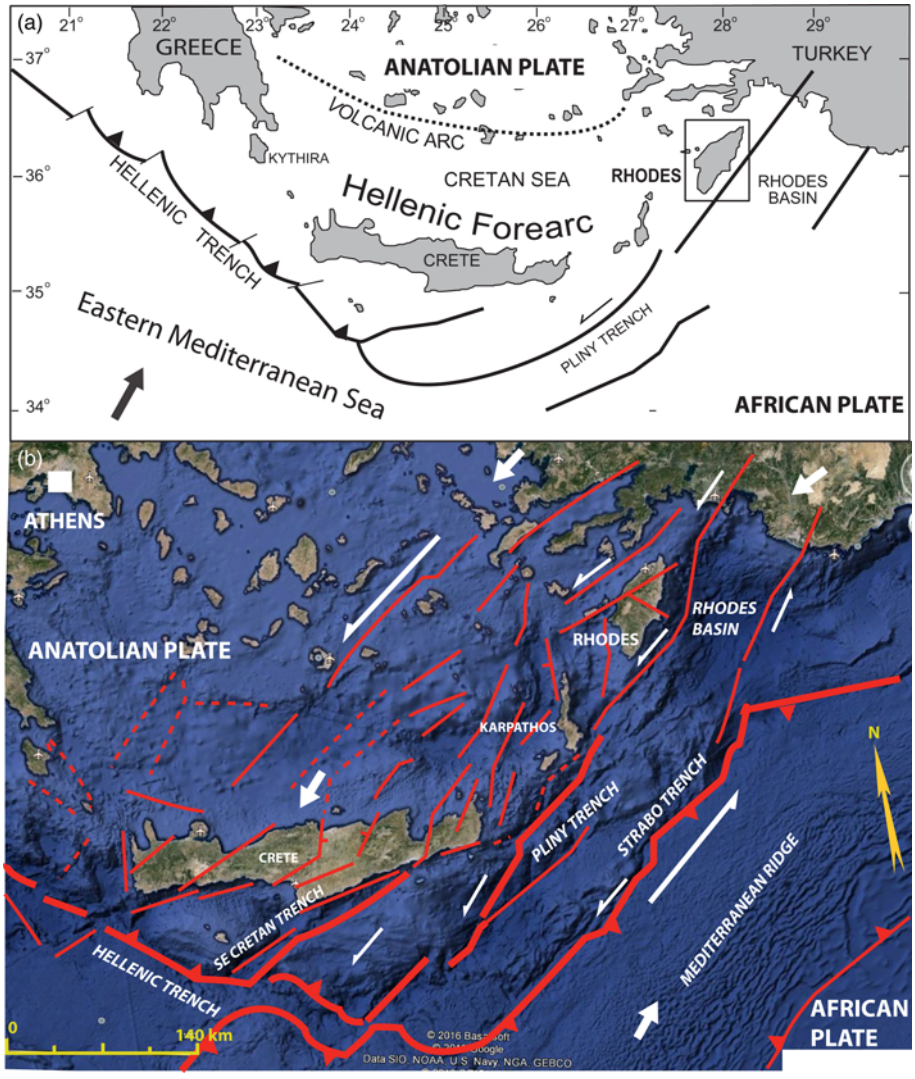

Fig. 1. (**a**) Location of Rhodes in the Aegean arc. (**b**) Active faulting in the Aegean arc during the Quaternary (from ten Veen 2004; ten Veen *et al.* 2009; Hall *et al.* 2009, 2014; Sakellariou *et al.* 2013; Tur *et al.* 2015). Background: Google Earth imagery. © 2016 Basarsoft, © 2016 Google. Data: SIO, NOAA, US Navy, NGA, GEBCO

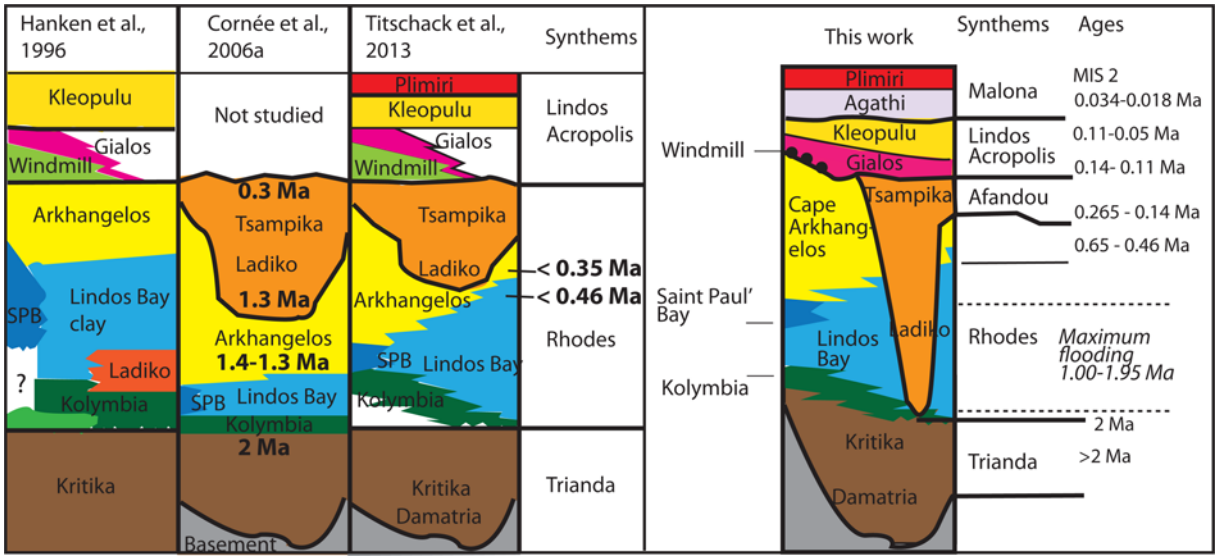

Fig. 2. Sketches of the proposed Quaternary lithostratigraphic successions of eastern Rhodes. SPB: Saint Paul's Bay Formation

(1996), several lithostratigraphic schemes were proposed, but the ages of the different lithological units and their spatial relationships are still debated (Hansen 1999; Cornée *et al.* 2006*a*; Titschack *et al.* 2008, 2013; Boyd 2009; Linse 2016) (Fig. 2). This is a result of the lack of strong chronostratigraphic constraints on the deposits, especially the shallow marine series, and the fact that the deposits cropping out along the eastern coast of Rhodes are patchily preserved in palaeovalleys that are mostly isolated one from each other. It is therefore not possible to use the entire Pleistocene sedimentary record to constrain the tectonic movements of Rhodes during this Epoch.

The Pleistocene deposits of Rhodes record three major transgressive–regressive cycles: the Trianda, Rhodes and Lindos-Acropolis synthems (Titschack *et al.* 2013).

The first cycle, the Trianda Synthem (*c.* 200 m maximum thickness), consists of continental (Damatria Formation) followed by brackish to shallow marine (Kritika Formation) siliciclastic sediments deposited in a muddy deltaic setting (Moissette *et al.* 2007, 2013, 2016). These formations were originally considered to be Piacenzian–Gelasian (Sissingh 1972; Benda *et al.* 1977) or Calabrian (Thomsen *et al.* 2001; Rasmussen *et al.* 2005). However, biostratigraphic analyses based on calcareous nannofossils have recently shown that the uppermost shallow marine part of the Kritika Formation was deposited during the late Gelasian (*c.* 2 Ma) (Moissette *et al.* 2016).

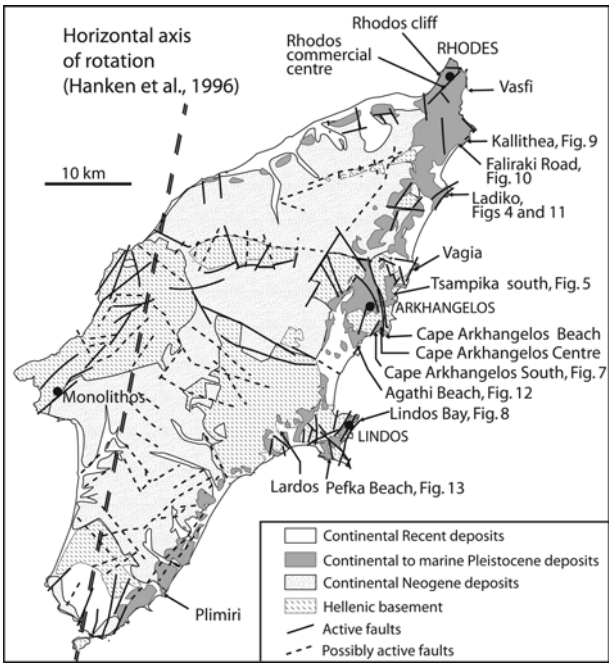

Fig. 3. Simplified geological map from Lekkas *et al.* (2000) showing the location of the investigated areas in eastern Rhodes.

The second cycle, the Rhodes Synthem (*c.* 420 m maximum thickness) is composed of: (1) littoral to lower offshore (Moissette & Spjeldnaes 1995; Steinthorsdottir *et al.* 2006; Steinthorsdottir & Hakansson 2017) bioclastic limestones of the Kolymbia Formation; (2) upper bathyal (Moissette & Spjeldnaes 1995; Rasmussen & Thomsen 2005; Milker *et al.* 2017) calcareous to silty clays of the Lindos Bay Formation; (3) deep sea coral boundstones (Hanken *et al.* 1996; Titschack *et al.* 2005) of the Saint Paul's Bay Formation; and (4) pluri-facies red algal and bryozoan-rich limestones and siliciclastic deposits (Hanken *et al.* 1996; Moissette *et al.* 2010; Titschack *et al.* 2013) of the Cape Arkhangelos Formation.

The yellowish bioclastic limestones of the Kolymbia Formation are organized in a back-stepping geometry. They are homogeneous throughout the outcrops, always argillaceous and yield a palaeontological content mainly composed of bryozoans, molluscs, echinoids and brachiopods, with rare or almost no red algae. The carbonate deposits of the Cape Arkhangelos Formation are organized in down-stepping clinoform units. They are dominantly composed of shallow water red algal and bryozoan boundstones with abundant serpulids when deposited on the Hellenic basement, changing basinwards into mollusc-, bryozoan- and red algae-rich bioclastic limestones, then into hemipelagic calcareous clays. The siliciclastic Ladiko Formation (Fig. 2) was first proposed to be stratigraphically located between the Kolymbia Formation and the Lindos Bay Formation (Hanken *et al.* 1996). Field relationships led Cornée *et al.* (2006*a*) to propose that it should be considered as the new Ladiko-Tsampika Formation, preserved in the palaeovalleys that eroded the Cape Arkhangelos Formation.

The age of the Kolymbia and Lindos Bay formations have long been debated (see Titschack *et al.* 2013; Quillévéré *et al.* 2016 and references cited therein). These recent studies, based on biostratigraphic analyses and the $^{40}Ar/^{39}Ar$ dating of biotite and plagioclase from volcanic ashes point to: (1) diachronous deposition of the transgressive Kolymbia Formation since the late Gelasian (calcareous nannofossil Zone CNPL7, 1.93–1.71 Ma) up to the earliest Calabrian (CNPL8, 1.71–1.25 Ma); (2) deposition of the Lindos

Bay Formation since the Late Gelasian (CNPL8, 1.71 Ma) up to the Ionian (CNPL10, *c*. 650 ka); and (3) diachronous deposition of the Cape Arkhangelos Formation during a forced regression, coeval with the deposition of the uppermost part of the Lindos Bay Formation at least since the interval corresponding to Zone CNPL10 (*c*. 1.00 Ma or later).

The age of the Cape Arkhangelos Formation is poorly established. It was supposed to have been deposited either during the Late Pleistocene (Hanken *et al*. 1996), during the Calabrian (1.3–1.4 Ma, Cornée *et al*. 2006*a*), from 108.6 ka during the latest Pleistocene (Nielsen *et al*. 2006), or to be locally younger than 650 ka to possibly 350 ka (Titschack *et al*. 2013).

Deposition of the Ladiko-Tsampika Formation was first estimated to have occurred between 1.3 and 0.3 Ma (Cornée *et al*. 2006*a*), but Boyd (2009) and Linse (2016) questioned the reliability of this lithostratigraphic unit based on macrofloral and mollusc associations, respectively. These researchers considered that the Ladiko-Tsampika Formation consisted of a peculiar facies of the Kritika Formation. The reliability and the age of the Ladiko-Tsampika Formation need to be revisited because the underlying Lindos Bay Formation has been proposed to have been deposited up to *c*. 600 ka ago at Lardos (Titschack *et al*. 2013).

The third cycle, the Lindos-Acropolis Synthem, was defined by Hanken *et al*. (1996) at Lindos Bay and complemented at Plimiri by Titschack *et al*. (2008). It consists of four formations. The Windmill Bay Formation is a local, frame-supported level of blocks of dismembered Cape Arkhangelos calcarenite (thickness <3 m). The blocks may be coated by stromatolites and bryozoans. They are embedded in a calcarenite. The Gialos Formation is a 3 m thick red algal boundstone. It was deposited during the Marine Isotope Stage (MIS) 6 to MIS 5e transgressive interval at Plimiri (between 140 and 110 ka; Titschack *et al*. 2008). The Kleopolu Formation is a coarse algal grainstone with cross-bedding, reaching a maximum thickness of 12 m at Lindos Bay (Hanken *et al*. 1996). It is also found at Plimiri (Titschack *et al*. 2008), where it was deposited during the MIS 5d to MIS 5a interval (between 110 and 71 ka). The Plimiri Formation, composed of aeolian sands, is considered to have been deposited during the glacial MIS 2 interval between 24 and 11 ka (Titschack *et al*. 2008).

We reinvestigated the upper part of the Rhodes Synthem and the Lindos-Acropolis Synthem based on field investigations of all the exposures available along the eastern coast of the island (Fig. 3) to establish clearer relationships between the different formations and to improve chronostratigraphic control.

Methods

We conducted several field mapping campaigns at a scale of 1:10 000 guided by Google Earth imagery. After the observation of thin sections, U/Th dating was performed on the best-preserved aragonitic part of six different shells of the bivalve species *Spondylus gaederopus* microdrilled in their inner part or hinge area (e.g. Maier & Tistschack 2010) (Supplementary data 1). These shells were collected, from the north to the south of the island, in sections at Ladiko Bay (samples LAD T and LAD Z), at Agathi Beach (samples SP AGA1 and SP AGA2), Lindos Bay (sample L2) and Pefka Beach (sample SP PEFE X) (Supplementary data 1; Fig. 3). Whenever possible and to avoid dating reworked samples, we sampled shells still attached to the basement (LAD T, SP AGA1, SP AGA 2 and PEFE X), but two samples were collected from a grainstone matrix (LAD W and L2). The analyses were performed using an AXIOM multi-collector inductively coupled plasma mass spectrometer at the GEOMAR Helmholtz Centre for Ocean Research Kiel, Germany, following the methodology described by Fietzke *et al*. (2005). As the U/Th dating on spondylids is an original attempt, the accuracy of our results is discussed in the Supplementary data. In all cases, the dates obtained were consistent with the stratigraphic relations between units inferred from field investigations. Foraminiferal biostratigraphic analyses were performed on four soft clayey samples from the Cape Arkhangelos Beach section. The samples were washed over a 65 μm screen. The residue was dry-sieved and the size fractions coarser than 125 μm were used to identify the taxa. For the analyses of the calcareous nannofossil biostratigraphy, we prepared standard smear slides of five and four soft clayey samples collected from the Cape Arkhangelos and Tsampika Beach sections, respectively (Supplementary data 2). The bio-event calibrations for planktonic forams and calcareous nannofossils are from Lourens *et al*. (2004) and Raffi *et al*. (2006), respectively, and we used the zonal scheme of Backman *et al*. (2012) for the calcareous nannofossils. Twenty thin sections originating from samples collected in the Faliraki Road, Lindos Bay, Agathi and Pefka Beach sections were prepared to better characterize the depositional environments of the indurated calcareous sediments, following the hydrodynamic classification synthetized by Merzeraud (2017).

Results

Rhodes Synthem

Cape Arkhangelos Formation

The proximal carbonate facies of the Cape Arkhangelos Formation unconformably rests above an erosional surface along the eastern coast of Rhodes (Fig. 3). Various types of rocks are found below this surface, including the calcareous Mesozoic–Paleogene basement (e.g. the Cape Arkhangelos, Ladiko and Kallithea areas), deposits of the Kritika Formation (e.g. Rhodes cliff) and deposits of the Kolymbia and Lindos Bay formations (e.g. Rhodes commercial centre, Vasfi, Cape Arkhangelos South, Agathi Beach and Lindos Bay). The clay-rich distal part of the Cape Arkhangelos Formation was locally found conformably overlying the upper part of the Lindos Bay Formation – for example, at Lardos (Titschack *et al*. 2013) and at Pefka Beach above a firmground (Quillévéré *et al*. 2016).

At Cape Arkhangelos, the prograding calcarenite at 70 m a.s.l. (Hanken *et al*. 1996) was found to laterally change southward into 4 m thick clay-rich limestone and clays. These more distal facies of the Cape Arkhangelos Formation were deposited at greater depth, allowing calcareous plankton biostratigraphic analyses. Such deposits are well exposed at Cape Arkhangelos Beach (36° 11′ 11.23″ N; 28° 7′ 59.35″ E), possibly overlain by the Kleopulu Formation. The clayey levels there yielded abundant *Amusium*, scaphopod and pteropod shells. All four collected samples yielded a well-preserved and diverse planktonic foram assemblage in which the most stratigraphically significant taxa were *Globoconella inflata* and *Globorotalia truncatulinoides excelsa*, which first occurred in the eastern Mediterranean at 2.09 Ma and 940 ka, respectively (Lourens *et al*. 2004). All four samples also yielded the benthic foram *Hyalinea balthica*, which first commonly occurred in the Mediterranean from 1.492 Ma (Lourens *et al*. 1998). We also note that the samples lacked sinistral morphotypes of *Neogloboquadrina* sp., whose last common occurrence in the eastern Mediterranean has been calibrated at 610 ka (Lourens *et al*. 2004), and the benthic foram *Stilostomella* sp., which became extinct in the Mediterranean between 700 and 580 ka (Weinholz & Lutze 1989; Kawagata *et al*. 2005). These data suggest that the clayey levels of the distal facies of the Cape Arkhangelos Formation outcropping in the Cape Arkhangelos Beach section deposited after 610 ka. This age estimate is further refined by the calcareous nannofossils. The common occurrence of *Gephyrocapsa caribbeanica* was identified in three samples. The first common occurrence of *G. caribbeanica* occurred in the 560–470 ka interval (e.g. Bollmann *et al*. 1998;

Flores *et al.* 1999; Baumann & Freitag 2004; López-Otálvaro *et al.* 2008). *Pseudoemiliana lacunosa*, whose last appearance datum occurred within MIS 12 at 458 ka (Thierstein *et al.* 1977), was found in all four samples.

We conclude from these biostratigraphic analyses that the distal clayey facies of the Cape Arkhangelos Formation section was deposited during the Ionian between 560 and 458 ka (upper calcareous nannofossil Zone CNPL10). It is not currently possible to definitely assign the age of the last deposits of the Cape Arkhangelos Formation because they were probably removed by erosion.

Ladiko-Tsampika Formation

The following new field observations were made in the Ladiko valley (Fig. 3).

(1) At Ladiko Pass, the northern side of the valley (Fig. 4a) shows deposits of the Kritika Formation truncated by an erosional surface (Fig. 4e). This surface is also found on the southern side of the valley along the road (Fig. 4g). Above the erosional surface, continental to shallow marine sandy to conglomeratic facies change eastward into shallow marine deposits (Ladiko Beach section).

(2) Several outcrops of basement limestones along the road to Ladiko are coated by relicts of red algal–bryozoan–serpulid boundstone to grainstone. Limestones resting unconformably on the basement along the eastern coast of Rhodes belong either to the Kolymbia Formation or to the Cape Arkhangelos Formation (Hanken *et al.* 1996; Cornée *et al.* 2006*a*). The relict limestones at Ladiko did not deliver useful microfossils for dating and their spatial relationships with the clays of the Lindos Bay Formation are unknown. Thus their stratigraphic position remains debatable. However, their facies is similar to that of the typical shallow water Cape Arkhangelos red algal boundstones to packstones found on the basement on the flanks of palaeovalleys, as, for example, around Profitis Ilias Mountain or in the Tsampika Beach area (Cornée *et al.* 2006*a*) and in numerous other areas of eastern Rhodes (e.g. Hanken *et al.* 1996; Hansen 1999). The transgressive limestones of the Kolymbia Formation often contain reworked fragments of the basement in their lower part and are mostly devoid of red algae (Cornée *et al.* 2006*a*; Steinthorsdottir *et al.* 2006; Steinthorsdottir & Hakansson 2017), except in some isolated outcrops of the Lindos area (Titschack *et al.* 2005). The relicts of the algal limestones found on the flanks of the Ladiko palaeovalley are consequently related to the deposits of the Cape Arkhangelos Formation and the deposits of the Ladiko-Tsampika Formation unconformably rest upon these relicts (Fig. 4b–d).

(3) Remnants of the Ladiko-Tsampika Formation are found stacked against the basement to the east inside a palaeovalley (Cornée *et al.* 2006*a*). Steep flanks with abundant borings delimit the palaeovalley (Hanken *et al.* 1996; Cornée *et al.* 2006*a*).

(4) We found a second carbonate deposit belonging to the Lindos-Acropolis Synthem unconformably above the Ladiko-Tsampika Formation (Fig. 4g).

To summarize, the Ladiko-Tsampika Formation was deposited above an erosional surface in a palaeovalley after the deposition of both the Kritika Formation and the Cape Arkhangelos Formation (surface 3 in Fig. 4g). We thus conclude that the Ladiko-Tsampika Formation is younger than the Cape Arkhangelos Formation.

A new road has been recently built at Tsampika Beach, the type locality of the Ladiko-Tsampika Formation, which was also found above relicts of red algal limestones of the Cape Arkhangelos Formation (Cornée *et al.* 2006*a*). The lower part of the Ladiko-Tsampika Formation (sedimentary cycles TSS1 and TSS2 in Cornée *et al.* 2006*a*) is particularly well exposed along this road (Fig. 5). From bottom to top, the section is composed of:

(1) 11 m thick reddish clays and sandstones resting above an erosional surface at the top of the basement (fluvial deposits);

(2) 2 m thick dark clays with shallow marine fauna (littoral deposits);

(3) 7 m thick sandstones and conglomerates with interbedded coal facies (alluvial fan deposits);

(4) 15 m thick greenish, laminated silty clays and a few limestones with marine fauna (lagoonal to upper offshore deposits that yielded *Bregmaceros* sp. fish remains); and

(5) 5 m thick sandstones and conglomerates above an erosional surface with venerid bivalves (uplifted beach deposits).

In sequence TSS 1 of the Tsampika Beach section (Fig. 5), calcareous nannofossils are poorly preserved and are reworked from the Miocene to Lower Pliocene (sample TSF1). The lower part of sequence TSS 2 (samples TSF 6–10; Fig. 5) yielded poorly to well-preserved assemblages, including rare representatives of *Gephyrocapsa omega* and common representatives of *P. lacunosa*, *P. ovata* and *Heliscophaera inversa* (Supplementary data 2). These indicate a late Pleistocene age (0.96–0.47 Ma) within calcareous nannofossil Zone CNPL10. Based on the common occurrence of *P. lacunosa* and *P. ovata*, combined with the absence of *Gephyrocapsa* sp., the age is probably younger than the td2 event of Cita *et al.* (2012) – the temporary disappearance of *G. omega* at *c*. 0.77 Ma. As a whole, the lower part of the sedimentary cycle TSS 2 could be assigned to the 0.77–0.47 Ma interval. Sample TSF 11, 4 m above TSF 10 (Fig. 5), yielded rare *Emiliania huxleyi* (Zone CNPL11).

At Cape Arkhangelos Centre (Fig. 3), patchy outcrops of greenish silty clays typical of the Ladiko-Tsampika Formation with debris flow interbeds are found unconformably resting against the basement (36° 12′ 21.1″ N; 28° 08′ 05.6″ E). Greenish clays yielded orbulinids and fish scales. The debris flows are composed of bored basement blocks to gravels associated with a transported littoral fauna (e.g. *Spondylus*, *Pecten* and oysters).

At Cape Arkhangelos South (Fig. 3), fresh exposures along the shoreline display, from bottom to top (e.g. 36° 11′ 15.7″ N; 28°07′ 25.4″ E; Fig. 6) the following beds.

(1) Calcareous basement, severely deformed, bored by lithophagid molluscs in its uppermost part.

(2) 1–3 m thick microconglomerate–carbonate–clays with debris flow interbeds displaying blocks reworked from the basement; oyster shells are often found. These deposits are clayey carbonates devoid of red algae. They contain reworked fragments from the basement in their lower part and onlap on the basement. Thus they can be confidently attributed to the transgressive Kolymbia Formation. About 50 m to the east along the shoreline (36° 11′ 16.71″ N; 28° 07′ 26.24″ E), these limestones are overlain by the pelagic grey clays of the Lindos Bay Formation, confirming their lithostratigraphic characterization.

(3) Carbonate–microconglomeratic beds (2–4 m thick) with some red algal and bryozoan debris, organized into metre-high clinoform beds that prograde to the south. These clinoforms rest on an erosional surface transecting the underlying clayey limestone of the Kolymbia Formation. All these features indicate that these beds correlate with the

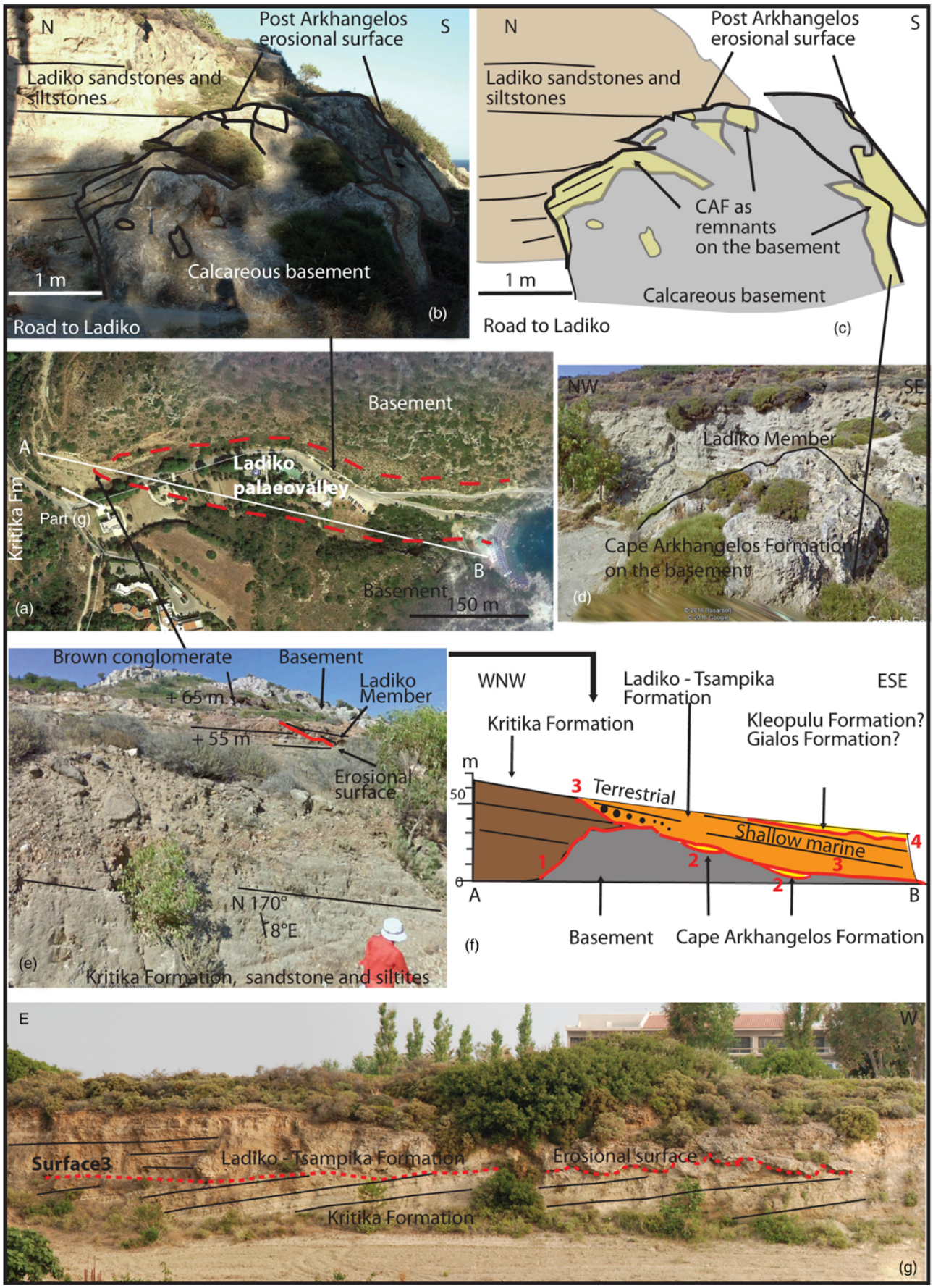

Fig. 4. Upper part of the Ladiko valley. (**a**) Location of the studied outcrops. (**b**, **c**) Calcareous basement overlain by relicts of red algal carbonates of the Cape Arkhangelos Formation and sealed by marine siliciclastic deposits of the Ladiko Formation. (**d**) Same outcrop, shown using Street View Google Earth imagery. © 2016 (**e** and **f**) The Kritika Formation is transected by an erosional surface overlain by proximal facies of the Ladiko Formation [(**e**) northern side of the valley; (**f**) southern side]. (**g**) Longitudinal cross-section of the Ladiko palaeovalley. CAF, Cape Arkhangelos Formation.

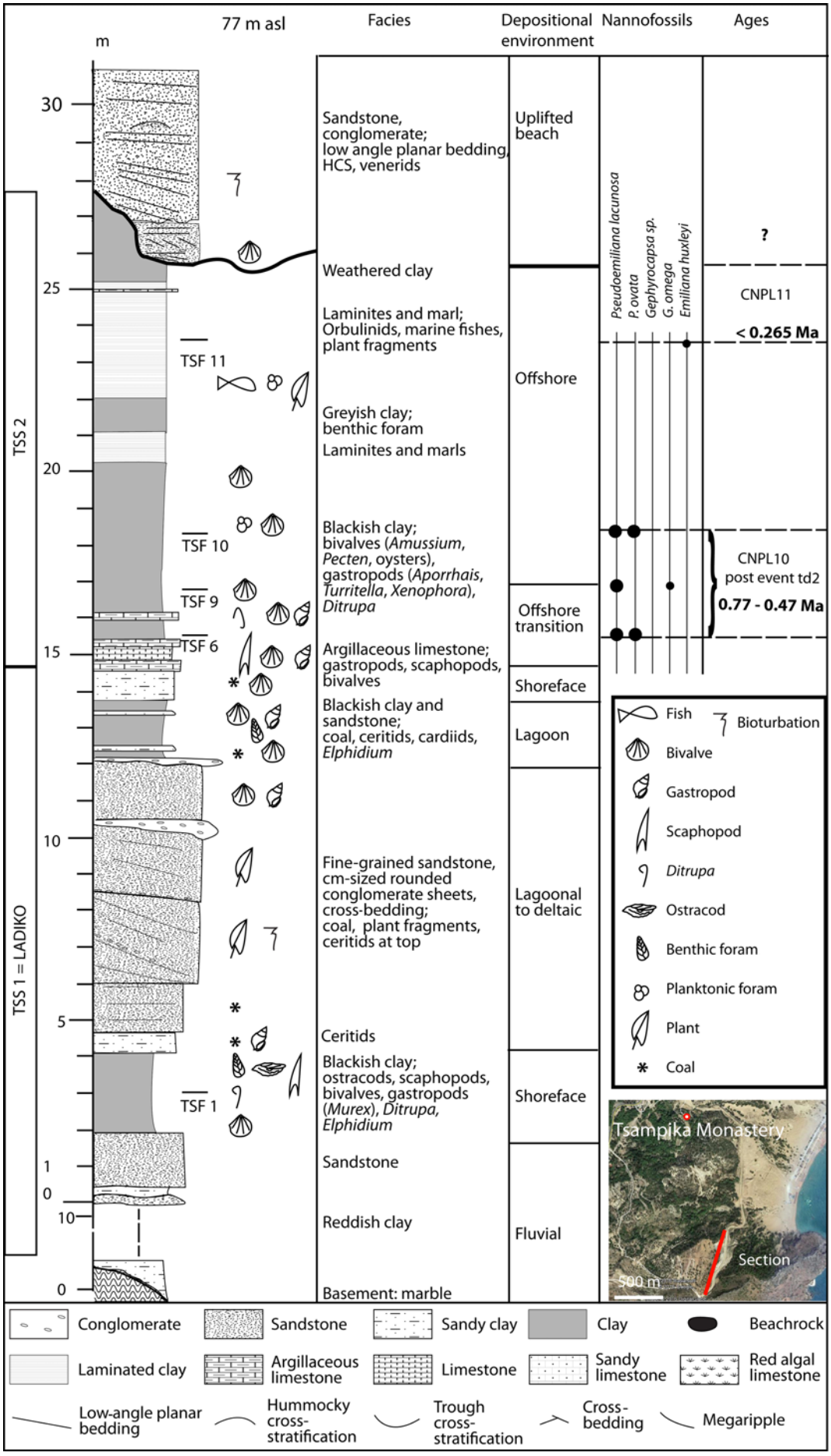

Fig. 5. Lithostratigraphic succession of sequences TSS1 and TSS 2 at Tsampika Beach, new road.

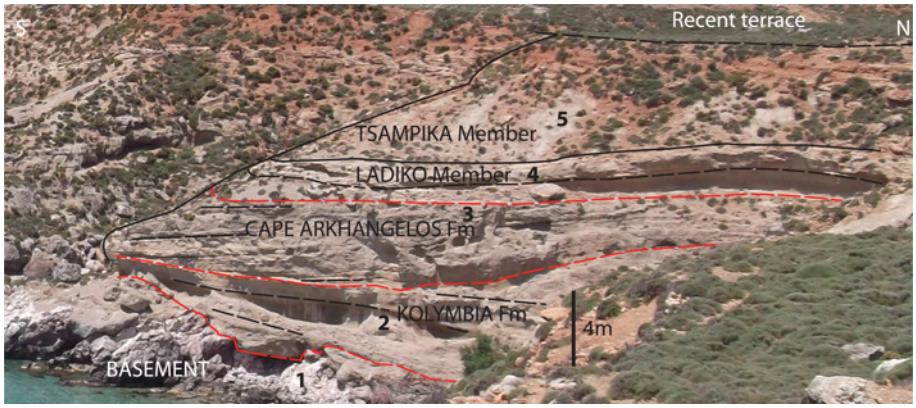

Fig. 6. Cape Arkhangelos South locality. The Ladiko-Tsampika Formation overlies the prograding Cape Arkhangelos Formation. Black lines (units 2–5), bedding; red lines, erosional surfaces. 1, calcareous basement; 2, sandy and clayey limestone and debris flows, Kolymbia Formation; 3, prograding sandy lime microconglomerate, Cape Arkhangelos Formation; 4, marine conglomerate to sandstone, Ladiko Member; and 5, greenish silty clays with orbulinids and fish scales, Tsampika Member.

Cape Arkhangelos Formation (note that the clays of the Lindos Bay Formation are missing here above the Kolymbia Formation).

(4) Microconglomerates (1–2 m thick) with transported oysters and some bored pebbles.

(5) Greenish laminated silty clays (4–5 m). The silty clays yielded orbulinids and poorly preserved calcareous nannofossils reworked from the Middle Miocene.

At this locality, the clinoform beds of the Cape Arkhangelos Formation (level 3) clearly appear unconformably overlain by sandy conglomeratic then greenish marine silty clay (levels 4 and 5) that can only be related to the Ladiko-Tsampika Formation.

Lindos-Acropolis Synthem

Lindos Bay

Hanken *et al*. (1996) defined the type locality of the Lindos-Acropolis Formation (Synthem in Titschack *et al*. 2013) at Lindos Bay (Fig. 7a). The down-stepping Cape Arkhangelos Formation is found above both the basement and the Lindos Bay Formation and lies on an erosional surface (Fig. 7b, d). The Cape Arkhangelos Formation extends eastward to a Roman quarry. Extensional, submeridian fractures occur in this area and part of the Cape Arkhangelos Formation is eroded (Fig. 7c). The top of the typical Cape Arkhangelos Formation (Fig. 7c) displays an irregular, smooth surface (Fig. 7d) with decimetre high reliefs shaped as metre-sized boulders and assigned to the Windmill Bay Formation (Fig. 7e, f). This surface shows crevasses and caves indicating subaerial erosion. In some cases, boulders can be totally individualized and separated from the underlying calcareous beds of the Cape Arkhangelos Formation.

The erosional surface is coated by centimetre thick carbonate crusts (Fig. 7e, f) of the Gialos Formation of Hanken *et al*. (1996), which is found above and between the boulders and on submarine palaeocliffs (Fig. 7h). These crusts are composed of <1 mm thick laminae displaying structures derived from microbial activity (peloidal to clotted micrite laminae, microdomes), rare serpulid worms and common shallow water encrusting bryozoans (Fig. 7g). Among these, the most abundant is *Onychocella angulosa*, associated with *Parellisina curvirostris*, *Figularia figularis* and *Schizoporella unicornis*. Scarce specimens of *Fenestrulina malusii*, *Cribrilaria* sp., *Annectocyma major*, *Hippaliosina depressa* and *Diplosolen obelium* are also found. Above the Gialos Formation, some decimetre thick sandy, coarse-grained lime rudstone of the Kleopulu Formation occur with red algae, molluscs, serpulids, bryozoans and calcareous pebbles bored by clionids (Fig. 7d). A moderately preserved spondylid shell (sample L2, Supplementary data 1) collected from the lowermost part of the deposits corresponding to the Kleopulu Formation provided a U/Th age of 86.7 ± 0.9 ka (late MIS 5).

To summarize, the Cape Arkhangelos Formation rests on the basement or the Lindos Bay Formation above an erosional surface. The Windmill Bay Formation represents an in-place chaotic deposit resulting from the subaerial exposure of the uppermost part of the Cape Arkhangelos Formation and sculpted by karstic erosion, followed by a marine invasion. The Gialos Formation corresponds to a shallow marine deposit with microbial, algal and bryozoan crusts, overlain by littoral facies of the Kleopulu Formation during the late part of MIS 5.

Kallithea–Faliraki road

In the Kallithea Beach section, the prograding sets of the Cape Arkhangelos Formation (Supplementary data 3, a) are well exposed (Hanken *et al*. 1996; Hansen 1999; Nielsen *et al*. 2006). The upper part of the cliff (Supplementary data 3, a, b) displays boulders similar to those found in the Windmill Bay Formation at Lindos Bay (Supplementary data 3, c). The Cape Arkhangelos Formation boulders result from more or less intensive karstic erosional processes (Supplementary data 3, d).

In this area, the Windmill Bay Formation is overlain by marine then continental deposits, which are well exposed in the neighbouring Faliraki Road section along the national road (Supplementary data 4). Above the tilted and eroded clays of the Lindos Bay Formation, we found, from bottom to top:

(1) 0.50 m thick conglomerates, beach rock slabs encrusted by red algae, spondylids and oysters (beach deposits);

(2) 4.50 m thick calcareous sandstones and microconglomerates with low-angle planar bedding topped by an erosional surface (upper shoreface deposits);

(3) 2.50 m thick calcareous sandstones and microconglomerates with both trough cross-bedding and cross-bedding (beach to upper shoreface deposits);

(4) 1 m thick conglomerate topped by an erosional surface (beach to emergence surface deposits);

(5) 3.50 m thick continental deposits with a reddish palaeosol with roots overlain by aeolianite then fluvial conglomerates (terrestrial deposits).

To summarize, the lowest 7.50 m of the deposits show the superimposition of two beach sequences, deposited above an erosional surface transecting the deposits of both the Lindos Bay Formation and the Cape Arkhangelos Formation. U/Th dating could not be realized due to severe diagenetic changes in the spondylid shells. The uppermost part of the section ends with continental deposits typical of the Plimiri Formation, which were probably deposited during the MIS 2 interval (Titschack *et al*. 2008).

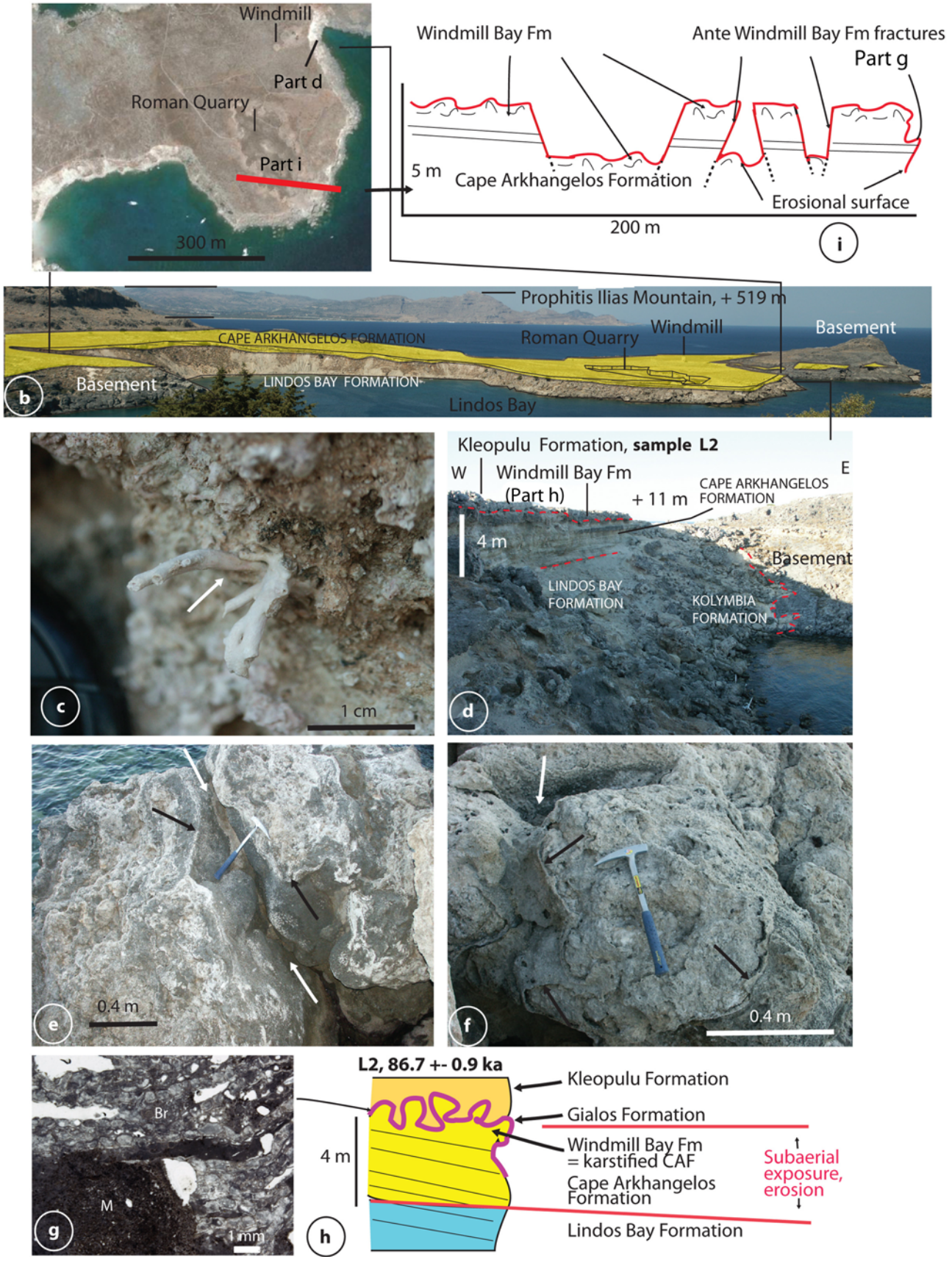

Fig. 7. Organization of the Pleistocene deposits in Lindos Bay, type locality of the Lindos-Acropolis Synthem. (**a**) Location. (**b**) The Cape Arkhangelos Formation rests on an erosional surface above both the Lindos Bay Formation and the basement. (**c**) Typical facies of the Cape Arkhangelos Formation with branching bryozoan. (**d**) The Windmill Bay Formation is the top of the Cape Arkhangelos Formation, which was more or less intensively dismembered by karstic processes. (**e**, **f**) Windmill Bay Formation: top of the Cape Arkhangelos Formation displaying karstic erosional features (white arrows) and coated by microbial crusts of the Gialos Formation (black arrows). (**g**) Microscopic view of the Gialos Formation with bryozoan crusts (Br) and clotted to peloidal micrite (microbial deposit, M). (**h**) Sketch of the Lindos-Acropolis Synthem deposits at Lindos Bay. (**i**) Cross-section of the quarry showing the faulted and eroded Cape Arkhangelos Formation; the Windmill Bay Formation constitutes the karstified top of the Cape Arkhangelos Formation. CAF, Cape Arkhangelos Formation.

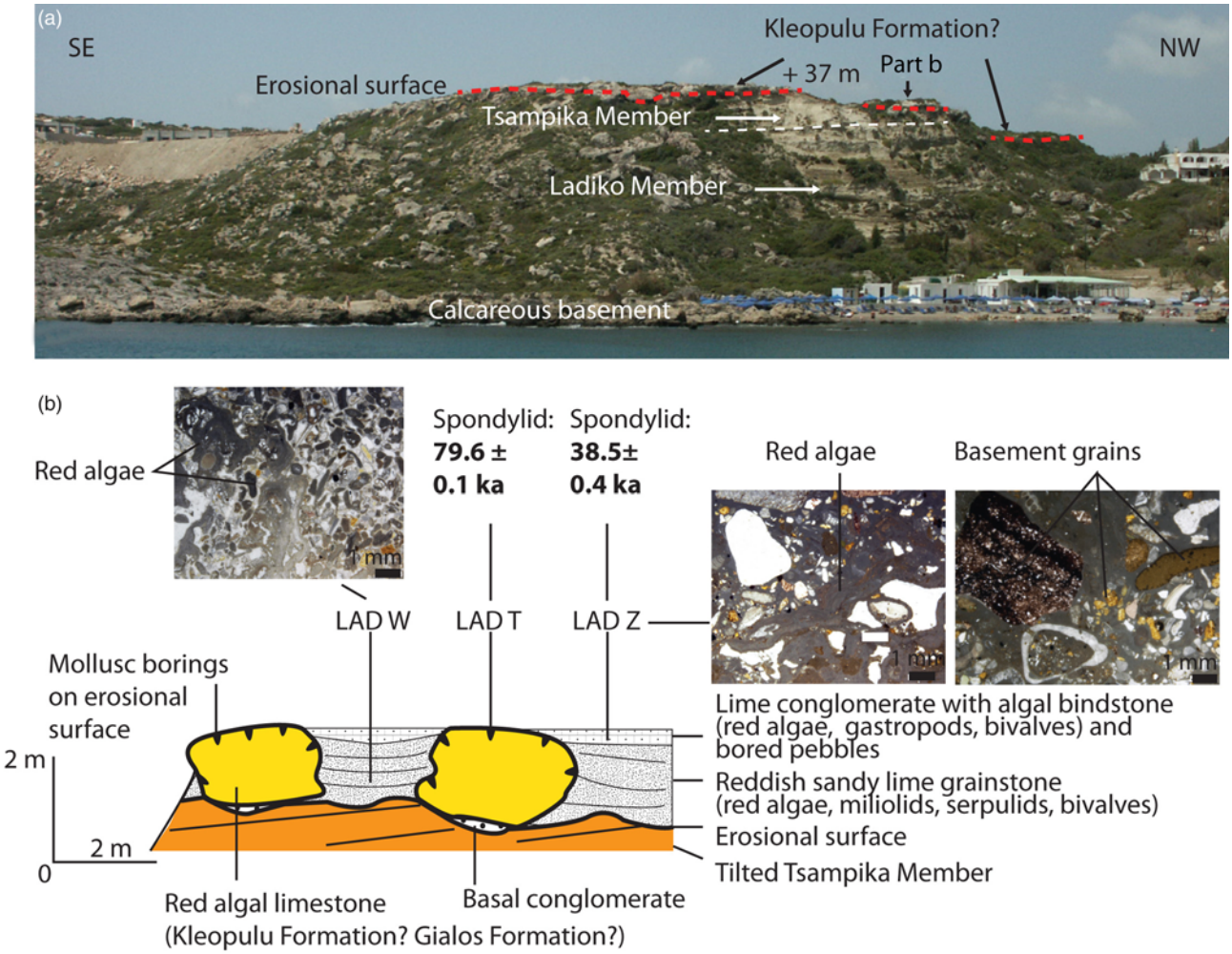

Fig. 8. Ladiko Beach section. (**a**) General view of the whitish calcarenite above the greenish silty clays of the Ladiko-Tsampika Formation. (**b**) Detailed view of lime boulders and sandy limestone infillings (with microscopic images).

Ladiko area

Deposits of the Ladiko-Tsampika Formation in the Ladiko valley (Fig. 4a) are overlain by whitish limestones above an erosional surface (Figs 4f & 8a). Above the seashore eastward, these limestones rest on the greenish shales of the Tsampika Member or on the basement; westward, they rest on different beds of the Ladiko-Tsampika Formation.

These white limestones, made of red algal boundstones, are similar to the MIS 5e limestones of the Gialos Formation described at Plimiri by Titschack *et al*. (2008). They locally crop out as metre-sized boulders bored by lithophagid molluscs, indicating that these limestone underwent erosion after deposition (Fig. 8b). The spaces between the boulders are infilled with littoral lime grainstones, then by lime conglomerates and red algal bindstones. A spondylid shell attached to the red algal boundstones (sample LAD T, Supplementary data 1) provided a U/Th age of 79.6 ± 1.0 ka. Another spondylid shell collected in the lime conglomerates above the erosional surface (sample LAD Z, Supplementary data 1) provided a U/Th age of 38.5 ± 0.4 ka.

Agathi Beach area

New exposures of limestones, sandstones and conglomerates were found above the Lindos Bay Formation in the southern part of the Agathi Beach between 4 and 21 m a.s.l. (36° 10′ 24.1″ N; 028° 05′ 56.5″ W; Fig. 9a).

From bottom to top, we found (Fig. 9b):

(1) 1–10 m thick red algal boundstones (coralligenous facies, lower shoreface deposits; Ballesteros 2006), topped by an erosional surface bored by lithophagid bivalves;
(2) 1–5 m thick scree composed of red algal boundstone boulders with the spaces between boulders infilled with a sandy lime grainstone (aerial scree then invaded by littoral deposits);
(3) 4 m thick bioturbated lime grainstones with megaripples and trough cross-bedding (upper shoreface deposits);
(4) 0.5 m thick conglomerate with boulders encrusted by red algae (beach rock deposits);
(5) 6 m thick siliciclastic lime deposits (shoreface to beach deposits).

Two spondylid shells, collected at 3.5 and 8.5 m in the section (samples SP AGA-1 and SP AGA-2, Supplementary data 1), were found attached on the erosional surface. They provided U/Th ages of 31.3 ± 0.2 and 17.8 ± 0.1 ka, respectively.

Pefka Beach area

Pleistocene deposits in the Pefka Beach area (Fig. 10a) are preserved in a narrow palaeovalley bounded by normal faults (Frydas 1994). In the lower part of the Pefka Beach section, the succession rests on the limestone basement and consists of, from bottom to top (Fig. 10b, c), clayey bioclastic limestones of the Kolymbia Formation, hemipelagic blue clays of the Lindos Bay Formation and bryozoan–mollusc lime wackestone to rudstone of the Cape Arkhangelos Formation

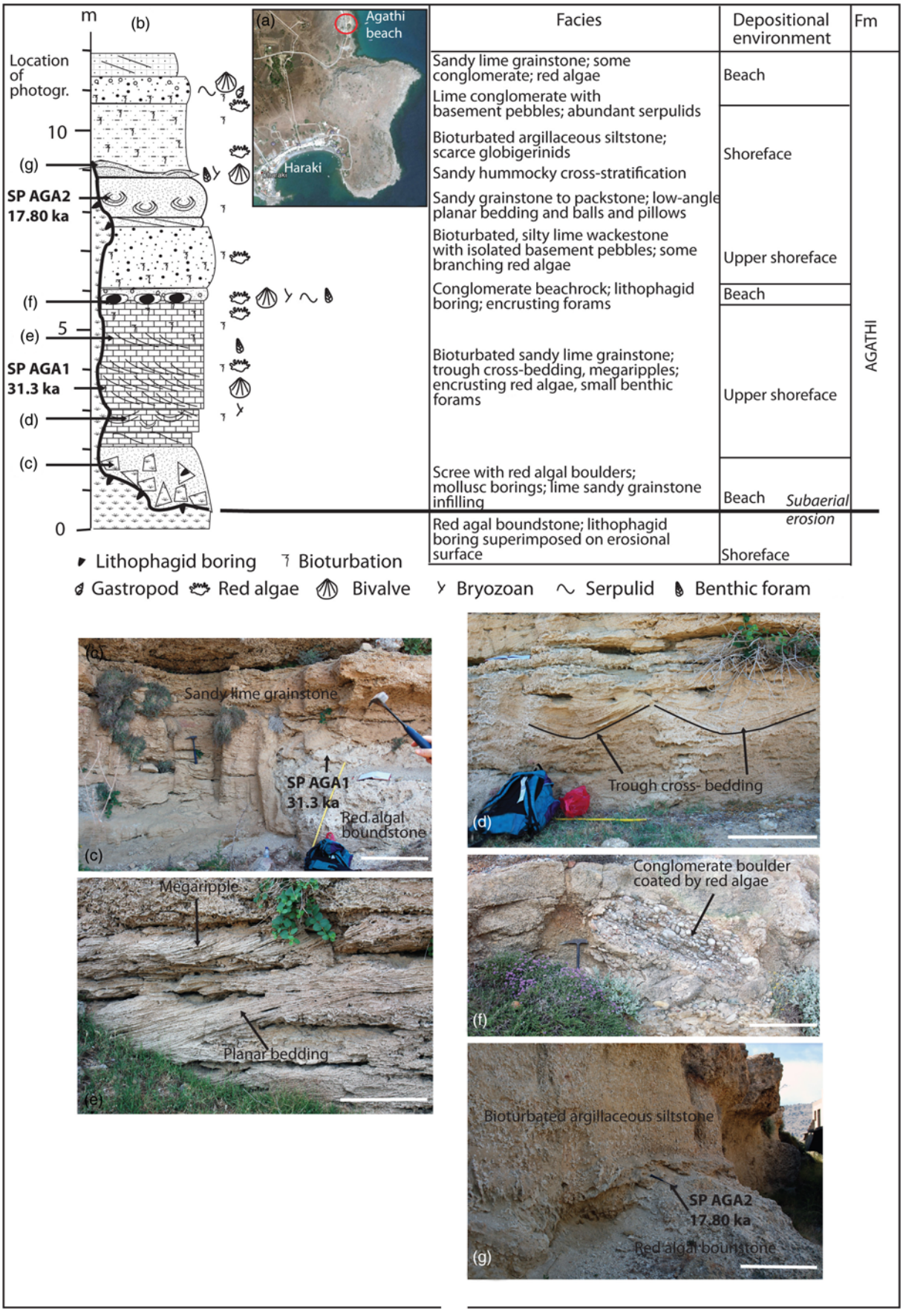

Fig. 9. Agathi Beach section. (**a**) Location. (**b**) Lithostratigraphy and depositional environment. (**c**) Location of sample SP AGA 1. (**d**) Trough cross-bedding. (**e**) Cross-bedding and megaripples. (**f**) Beachrock with conglomeratic boulders. (**g**) Location of sample SP AGA 2. Scale bar 0.5 m. Legend for lithology and sedimentary structures as in Figure 5.

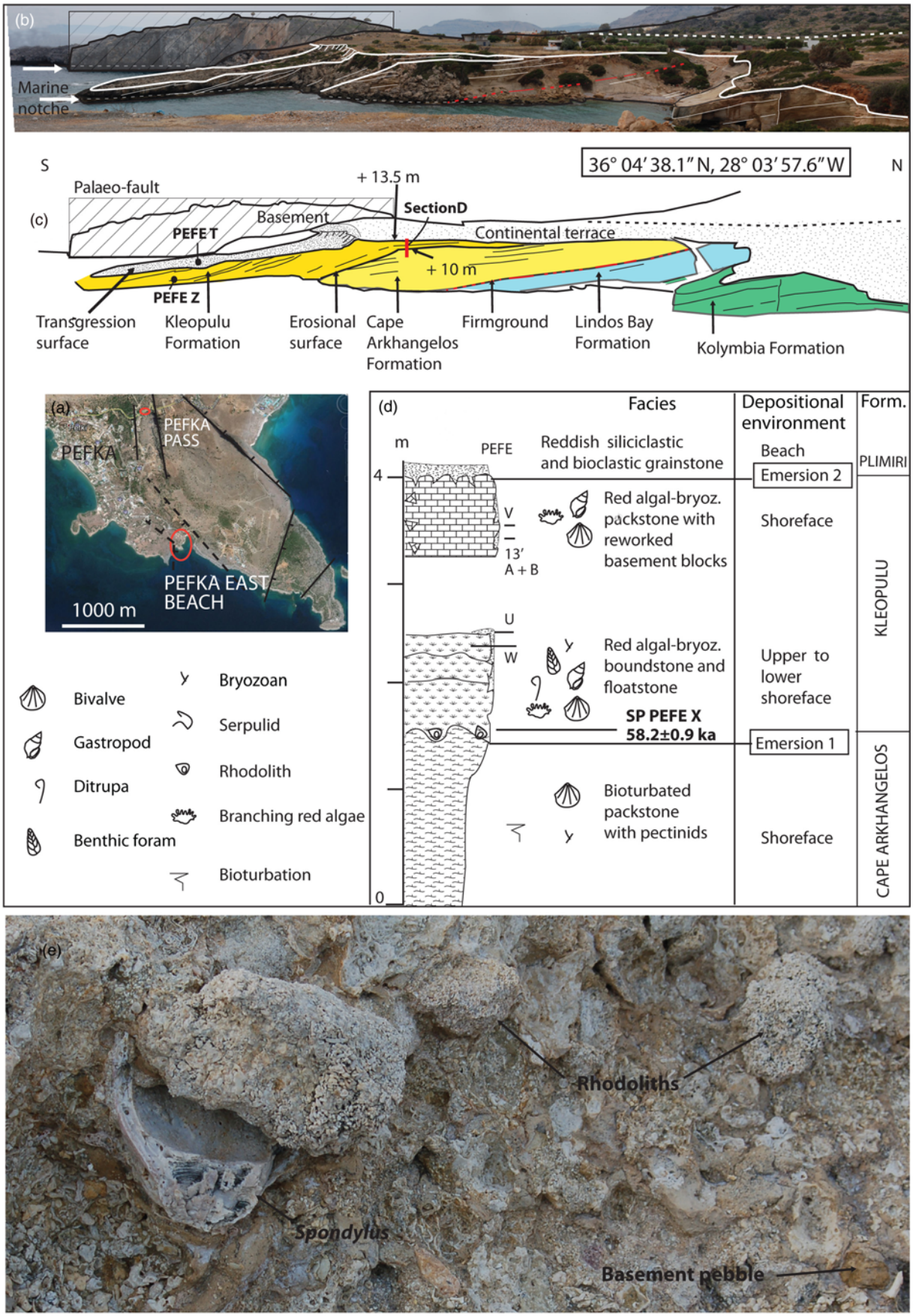

Fig. 10. Pefka Beach. (**a**) Location (Google Earth, © 2016). (**b**) Field view. (**c**) Interpretation of the field view. (**d**) Section of the whitish limestone above the Cape Arkhangelos Formation. (**e**) Coralligenous facies with rhodoliths and spondylids, lower part of section D. Legend for lithology and sedimentary structures as in Figure 5.

(Quillévéré *et al.* 2016; Milker *et al.* 2017). These deposits encompass calcareous nannofossil Zones CNPL7 to CNPL9 between 1.9 and 1.0 Ma (Quillévéré *et al.* 2016). Deposits of the Cape Arkhangelos Formation are topped by an erosional surface (Fig. 10b, c).

Above this surface, the succession displays whitish limestones with, from bottom to top (Fig. 10d):

(1) 1 m thick red algae and bryozoan-rich boundstone to floatstone with rhodoliths, serpulids, *Ditrupa* worms, gastropods (*Turbo*), spondylids, solitary corals, miliolids and grains reworked from the basement (coralligenous facies, shoreface deposits). The lowermost part of the deposits consists of red algal–mollusc rudstone. An attached, well-preserved spondylid shell yielded a U/Th age of 58.2 ± 0.9 ka (sample SP PEFE X, Supplementary data 1).
(2) 1 m without exposure;
(3) 0.8 m thick red algal–bryozoan lime packstone, with bivalves and gastropods (coralligenous facies, shoreface deposit);
(4) centimetre to decimetre thick reddish siliciclastic and bioclastic lime grainstone with red algae, molluscs, serpulids and miliolids (littoral deposit) deposited above an erosional surface (Fig. 10d).

The whitish limestone changes southwards into 5 m thick prograding lime grainstone and red algal–bryozoan boundstone, with echinoids, gastropods and scarce globigerinids (PEFE T and Z, Fig. 10b). The top of the deposits is eroded and bored by lithophagid bivalves and is overlain by reddish siliciclastic and bioclastic lime grainstone.

Discussion

Age model

Rhodes Synthem

Titschack *et al.* (2013) (at Lardos) and Quillévéré *et al.* (2016) (in multiple sections of the eastern coast of Rhodes) showed that the ages of the Kolymbia Formation and Lindos Bay Formation are late Gelasian to earliest Calabrian (CNPL6 to CNPL7) and late Gelasian to early Ionian (CNPL7 to CNPL10, 2 to *c.* 0.65 Ma), respectively (Fig. 11). They showed that the limestone facies of the Kolymbia Formation might laterally change into clays of the Lindos Bay Formation. They also proposed that part of the overlying erosive proximal carbonates of the Cape Arkhangelos Formation might laterally change into more distal clay-rich facies resembling those of the Lindos Bay Formation. Previous studies were, however, unable to provide firm chronostratigraphic constraints on the deposition of the Cape Arkhangelos Formation.

We show here that the common occurrence of *G. caribbeanica*, together with the occurrence of *P. lacunosa* and the absence of *E. huxleyi* in the Cape Arkhangelos Beach section (the later taxon also missing at Lardos; Titschack *et al.* 2013), indicate that the uppermost part of the Cape Arkhangelos Formation was deposited during the Ionian between 560 and 458 ka (late calcareous nannofossil Zone CNPL10). This age is older than that proposed at Lardos Hill by Titschack *et al.* (2013), who considered that the transition between the Lindos Bay Formation and the siliciclastic Cape Arkhangelos occurred at *c.* 350 ka.

Ladiko-Tsampika Formation

At Ladiko, Tsampika Beach and Cape Arkhangelos, the Ladiko-Tsampika Formation unconformably rests either on an erosional surface, on the basement, the Kritika Formation, or the Cape Arkhangelos Formation. It is therefore clearly younger than the Cape Arkhangelos Formation deposited between 560 and 458 ka. At Tsampika Beach the nannofossils found in Sequence TSS2 dating the 0.77–0.47 Ma interval (Fig. 5) are probably reworked because: (1) they indicate the age of the underlying upper Lindos Bay and Cape Arkhangelos formations deposits, topped by an erosional surface; and (2) sample TSF 11, 4 m above TSF 10 (Fig. 5), yielded rare *E. huxleyi* (Supplementary data 2), indicative of calcareous nannofossil Zone CNPL11 (the first occurrence of *E. huxleyi* occurred at 0.265 Ma in the eastern Mediterranean; Lourens *et al.* 2004). We thus conclude from these biostratigraphic analyses that the greenish laminated clays of sequence TSS2 within the Ladiko-Tsampika Formation were deposited at the earliest between 0.77 and 0.47 Ma, but probably during the late Ionian or Late Pleistocene, after 0.265 Ma. At the top, the Ladiko-Tsampika Formation is overlain by the Gialos Formation, the deposition of which began during MIS 5e at *c.* 114 ka and was deposited during the MIS 7 interval (Fig. 11). The Ladiko-Tsampika Formation should no longer be related to part of the Gelasian Kritika Formation, as still considered by Boyd (2009) and Linse (2016).

Lindos-Acropolis Synthem

Deposits of the Windmill Bay Formation are scarce. They mainly occur at Lindos Bay and Kallithea and we found some small-extent outcrops at Cape Vagia and Vasfi. These deposits always crop out below the Gialos Formation or below younger beach facies deposits. Deposits of the Windmill Bay Formation are composed of separated metre-sized boulders originating from the uppermost part of the calcarenite of the Cape Arkhangelos Formation. These blocks result from an on-site, karstic dismantling of the Cape Arkhangelos Formation during a period of emersion. This episode occurred between the deposition of the marine Ladiko-Tsampika Formation and the Gialos Formation, probably at least partly during the low sea-level interval corresponding to MIS 6 (Fig. 11).

The Gialos Formation is either composed of shallow water microbial–bryozoan crusts (Lindos Bay) or of red algal boundstones in deeper settings where they were dated between 140 and 110 ka (Plimiri; Titschack *et al.* 2013). The red algal boundstones at Ladiko were deposited on a major erosional surface transecting the Ladiko-Tsampika Formation (surface 4 in Fig. 4). At the top, the red algal boundstones are transected by an erosional surface, prior to the settlement of spondylids at 79.6 ± 0.1 ka (Fig. 8b). They are related to the Gialos Formation (MIS 5e) or the Kleopulu Formation (MIS 5a to d) (Titschack *et al.* 2008). These deposits consequently emerged and were eroded into boulders prior to the deposition of the coarse-grained littoral deposits in the *c.* 80–34 ka interval (levels LAD W and T on Fig. 8b; MIS 5a to MIS 3 interval). These littoral deposits, which lie above an erosional surface and are clearly younger than the Kleopulu Formation (110–71 ka; Titschack *et al.* 2008), are assigned to a new lithostratigraphic unit. Our study suggests that the red algal facies of the Gialos Formation are also present at Agathi Beach (Fig. 9b) and Tsampika (Cornée *et al.* 2006*a*).

The littoral coarse-grained deposits of the Kleopulu Formation, at Lindos Bay, formed at *c.* 86.7 ± 0.9 ka during the late part of MIS 5 (Fig. 7b). At Ladiko, spondylids attached on the previously eroded Gialos Algal Biolithite Formation provided a U/Th age of 79.6 ± 0.1 ka (Fig. 8b). At Pefka Beach, 2–5 m thick red algal–bryozoan boundstone to floatstone deposited above the Cape Arkhangelos Formation on an erosional surface and an attached spondylid yielded an age of *c.* 58.2 ± 0.9 ka (Fig. 10d). Together, these data from different localities indicate that the Kleopulu Formation deposited from the late part of MIS 5 to the earliest part of MIS 4 (Fig. 11), a time interval similar to that estimated at Plimiri for the deposition of the Kleopulu Formation (110–71 ka; Titschack *et al.* 2008). The mostly coastal deposits of the Kleopulu Formation are topped by an erosional surface that

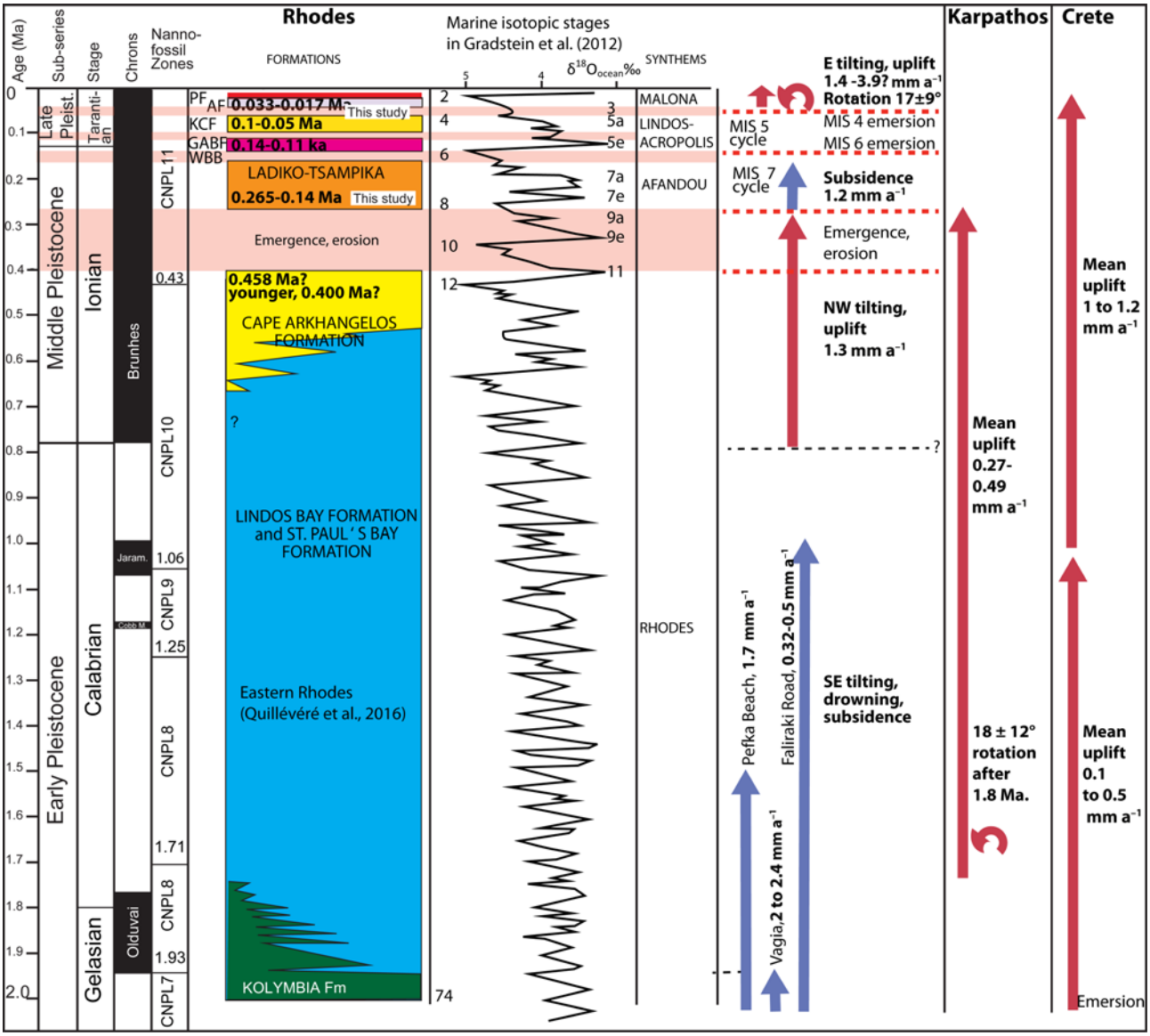

Fig. 11. Age model for the Pleistocene deposits of eastern Rhodes and tectonic motions in Rhodes, Karpathos and Crete since the Late Gelasian. AF, Agathi Formation; GABF, Gialos Formation; KCF, Kleopulu Formation; PF, Plimiri Formation; WBB, Windmill Bay Formation. LR04-stack from Lisiecki & Raymo (2005). Tectonic motions: Rhodes, van Hinsbergen *et al.* 2007, this work; Karpathos, van Hinsbergen 2004; Duermeijer *et al.* 2000; Moissette *et al.* 2017; Crete, Meulenkamp *et al.* 1994; Duermeijer *et al.* 1998, 2000; Roberts *et al.* 2013; Strobl *et al.* 2014.

formed between the late part of MIS 5 and MIS 3. They are thus probably related to the low sea-level that occurred during MIS 4, which has been estimated between *c.* 90 and 110 m b.s.l. (e.g. Rohling *et al.* 2017).

Agathi Formation: a new lithostratigraphic unit

At Tsampika (Fig. 5), Faliraki Road (Supplementary data 4), Ladiko (Fig. 8), Agathi Beach (Fig. 9) and Pefka Beach (Fig. 10), coarse-grained, siliciclastic–carbonate deposits from beach to upper shoreface settings are patchily preserved either above the Lindos Bay Formation, the Ladiko-Tsampika Formation, the Windmill Bay Formation, the Gialos Formation or the Kleopulu Formation, systematically resting above a subaerial erosional surface. They are consequently younger than the latest part of MIS 5. Where outcrops are well preserved (in the Faliraki Road and Agathi Beach sections), these deposits display two superimposed beach sequences. At Ladiko, the analysed spondylid shell provided a U/Th age of *c.* 38 ka (Fig. 8). At Agathi Beach, the lower and upper beach sequences provided U/Th ages of *c.* 31 and 18 ka (Fig. 9), respectively. At Faliraki (Supplementary data 4), these beach to upper shoreface deposits are overlain by continental deposits similar to those of the MIS 2 Plimiri Formation of Titschack *et al.* (2008). We conclude that these beach to upper shoreface deposits characterize a new lithostratigraphic unit named the Agathi Formation from the reference Agathi Beach section (Fig. 9). The Agathi Formation deposited during the Late Pleistocene within the late part of MIS 3, between *c.* 38 and *c.* 18 ka (Fig. 11).

Sedimentary cycles

The Rhodes Synthem is a long-term transgressive–regressive cycle ending with a major forced regression resulting in the deposition of the Cape Arkhangelos Formation (e.g. Hanken *et al.* 1996; Cornée *et al.* 2006*a*; Titschack *et al.* 2013 and references cited therein) (Fig. 12). The emergence period that occurred between the deposition of the Cape Arkhangelos and Ladiko-Tsampika formations for lasted a maximum of *c.* 200 ka (Fig. 11).

The Ladiko-Tsampika Formation displays a transgressive–regressive cycle, with first the deposition of the continental to shallow marine Ladiko Member (sequence TSS 1 of Cornée *et al.* 2006*a*), then the superimposition of at least seven other transgressive–regressive cycles

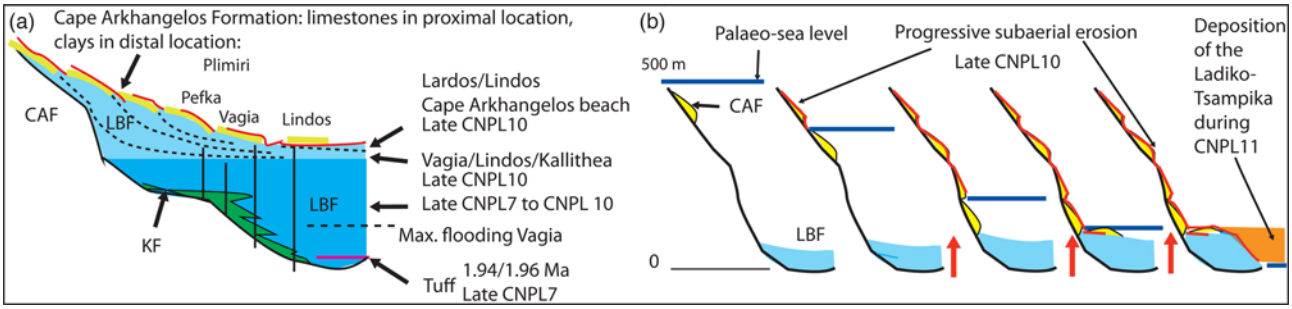

Fig. 12. Vertical motions during deposition of the Rhodes Synthem. (**a**) Reconstruction of the global architecture of the Rhodes Synthem. (**b**) Forced regression corresponding to the deposition of the Cape Arkhangelos Formation. CAF, Cape Arkhangelos Formation; KF, Kolymbia Formation; LBF, Lindos Bay Formation.

of higher order (Tsampika Member; sequences TSS 2 to TSS 8; Cornée *et al.* 2006*a*; Joannin *et al.* 2007) and topped by an emergence unconformity. The Ladiko-Tsampika Formation was emplaced during the interval corresponding to MIS 7, between *c.* 265 ka and *c.* 140–130 ka (Fig. 11). The eight TSS sequences of the Ladiko-Tsampika Formation, first assigned to *c.* 100 ka eccentricity controlled cycles (Cornée *et al.* 2006*b*; Joannin *et al.* 2007), are now assigned to *c.* 20 ka precession-controlled cycles. Outcrops of the Ladiko-Tsampika Formation are scarce along the eastern coast of Rhodes because the formation has most often been eroded. Nevertheless, they are patchily found along a 20 km transect in the southeastern part of the island (Ladiko valley, Tsampika Beach and Cape Arkhangelos area), bounded at the bottom and top by regionally identified subaerial erosional surfaces. Thus the Ladiko-Tsampika Formation should be related to a Synthem according to the International Guide of Stratigraphy (Salvador 1994), which we call the 'Afandou Synthem' (Afandou village is situated between Tsampika Beach and the Ladiko valley). The deposits of the Ladiko-Tsampika Formation were emplaced into coastal, beach to upper offshore settings (Cornée *et al.* 2006*a*) at an estimated palaeodepth ranging from 0 to *c.* 60 m. During MIS 6, the sea-level was between 60 and 120 m below the present day sea-level (e.g. Rohling *et al.* 2017) and we believe that the regional erosional surface found at the top of the Ladiko-Tsampika Formation may be related to this lowstand MIS 6 interval.

Deposits of the Lindos-Acropolis Synthem (Hanken *et al.* 1996) have previously been assigned to a unique transgressive–regressive sedimentary cycle extending from MIS 5e to MIS 2 (the Gialos Formation to the Plimiri Formation; Titschack *et al.* 2013) (Fig. 11). The newly defined Agathi Formation, which apparently deposited during the MIS 3 interval, allows us to refine this interpretation. The Lindos-Acropolis Synthem is restricted to the MIS 5 Gialos and Kleopulu formations, both topped by a MIS 4 erosional surface found patchily preserved at Plimiri, Pefka Beach, Agathi Beach, Tsampika South, Ladiko and Faliraki Road. Thus the extent of this surface is clearly of regional significance because it is found along 60 km of the eastern coast of Rhodes. The transgressive–regressive nature of the overlying sedimentary cycle, which resulted in the deposition of the marine Agathi Formation and then the continental Plimiri Formation, allows the definition of a new synthem called the Malona Synthem (Malona village is situated a few kilometres west of Agathi Beach).

Tectonic movements

Rhodes Synthem

During the deposition of the Kolymbia and Lindos Bay formations, Rhodes was tilted to the south, triggering drowning of its eastern coast (e.g. Hanken *et al.* 1996; Kovacs & Spjeldnaes 1999; Cornée *et al.* 2006*a*; van Hinsbergen *et al.* 2007). The global distribution of the facies in the palaeovalley system of Rhodes displays a complicated pattern (Titschack *et al.* 2013) (Fig. 12a). The transgression of the synthem began during the late Gelasian at *c.* 2 Ma within calcareous nannofossil Zone CNPL7 (Fig. 12a). In the Pefka Beach section, Milker *et al.* (2017) estimated palaeodepths reaching *c.* 850 m at *c.* 1.47 Ma. This drowning lasted for *c.* 500 ka, indicating mean subsidence rates of *c.* 1.7 mm a^{-1}. At Cape Vagia, the drowning of Rhodes was found to reach maximum palaeodepths of 300–600 m (bryozoan studies; Moissette & Spjeldnaes 1995) or *c.* 500–600 m (foram studies; van Hinsbergen *et al.* 2007) in laminated clays of the Lindos Bay Formation 6 m above the base of the section. There, maximum drowning occurred during the early Calabrian at *c.* 1.75 Ma within the earliest part of Zone CNPL8 (Quillévéré *et al.* 2016) (Fig. 11). Such a palaeodepth is consistent with the location of the highest marine terraces of the Rhodes Synthem in the Cape Arkhangelos area at 519 m a.s.l. (Cornée *et al.* 2006*a*) (Fig. 12b). Using a 500–600 m palaeodepth reached during *c.* 250 ka, an apparent subsidence rate of 2–2.4 mm a^{-1} can be calculated. In the uppermost part of the Faliraki Road section in the NE of Rhodes, Rasmussen & Thomsen (2005) estimated maximum palaeodepths of 360–480 m in levels that were deposited between 1.12 and 0.96 Ma (Quillévéré *et al.* 2016). Thus the rate of drowning here is estimated to be in the 0.32–0.5 mm a^{-1} interval. In summary, palaeodepths reached hundreds of metres when the hemipelagic clays of the Lindos Bay Formation were deposited. Nevertheless, even if the paleodepth estimates are subject to uncertainties, both the timing of maximum drownings and their amplitude clearly vary between the Pefka Beach, Cape Vagia and Faliraki Road sections. This indicates that the eastern part of Rhodes was not drowned as a single block with only one synchronous maximum drowning surface. Rather, differential and diachronous vertical motions occurred from the south to the north of the island. Future palaeobathymetric estimations from numerous other exposures of the Lindos Bay Formation may further constrain this history.

The forced regression that triggered the deposition of the Cape Arkhangelos Formation began during the late Calabrian within the late part of Zone CNPL9 based on recent dating by Titschack *et al.* (2013), Quillévéré *et al.* (2016) and this work (Fig. 12a, b). During the latest Calabrian–early Ionian (Zone CNPL10), a shallowing trend was observed at Lindos Bay, Cape Vagia and Lardos (e.g. Moissette & Spjeldnaes 1995; Titschack *et al.* 2013). The carbonates of the Cape Arkhangelos Formation alternately deposited and emerged (Cornée *et al.* 2006*a*) and a final emergence occurred during the middle Ionian in the levels correlating with the late part of Zone CNPL10. The uppermost terraces were probably removed as a result of current erosion and karstification. In the Cape Arkhangelos area, these terraces are stepped from between 519 m a.s.l. and 0 m (Cornée *et al.* 2006*a*), covering a time span of *c.* 400 ka (Fig. 11). The apparent mean uplift rate is consequently *c.* 1.3 mm a^{-1}. This rate is lower than previous estimates of *c.* 5 mm a^{-1} (Cornée *et al.* 2006*a*) or *c.* 2.5 mm a^{-1} (Joannin *et al.* 2007).

Afandou Synthem subsidence

The coastal palaeovalleys that were formed during the Cape Arkhangelos Formation forced regression were filled with deposits of the Ladiko-Tsampika Formation during the MIS 7 interval (Fig. 12). At Tsampika Beach, these deposits consist of at least eight coastal sequences reaching 147 m a.s.l. (Cornée *et al*. 2006*a*). All eight sequences deposited during a maximum duration of 125 ka (Fig. 11). The minimum apparent subsidence rate is therefore estimated as *c.* 1.2 mm a^{-1} (Fig. 11). When subsidence stopped, deposits of the Ladiko-Tsampika Formation emerged and were eroded during the lowstand corresponding to the MIS 6 interval. Later, littoral marine deposits again invaded the eastern coast of Rhodes during MIS 5 (Lindos-Acropolis Synthem).

Post-MIS 3 uplift

The deposits of the Malona Synthem were emplaced during MIS 3. The high sea-level that occurred during MIS 3 was at *c.* 40–90 m below the present day sea-level (Rohling *et al*. 2017). Today, deposits of the MIS 3 interval are found between 5 and 20 m a.s.l. at Agathi Beach, at 36–37 m a.s.l. at Ladiko and between 15 and 25 a.s.l. at Faliraki Road. The deposits of the Malona Synthem were consequently differentially uplifted along the eastern coast of Rhodes. Using the lowest beach facies of the deposits, the minimum uplift is 45 m at Agathi (5 m of elevation and a minimum of 40 m sea-level change) and the maximum is 127 m at Ladiko valley (37 m of elevation and a maximum of 90 m sea-level change) since 33 ka. Thus the apparent uplift rate is broadly estimated to be between 1.4 and 3.9 mm a^{-1}. This post-MIS 3 uplift includes the Holocene uplift of Rhodes, reaching 3.75 m elevation in the northernmost part of the island and decreasing to zero in its southern part, related to a westward tilt of the island (Pirazzoli *et al*. 1989; Hanken *et al*. 1996; Kontogianni *et al*. 2002). The Holocene uplift should be related to the activity of the thrust fault images from offshore seismic investigations below Rhodes (Woodside *et al*. 2000; Kontogianni *et al*. 2002; Hall *et al*. 2009).

Rotations around vertical axis

Duermeijer *et al*. (2000) found that Rhodes experienced an average anticlockwise rotation of 18 ± 12° since *c.* 1.8 Ma, but the studied sites were poorly dated. New investigations were conducted by van Hinsbergen *et al*. (2007) based on the revised chronostratigraphy of Cornée *et al*. (2006*a*). From this study, the island experienced two phases of counterclockwise rotation, 9 ± 6° between 2.5 and 1.8 Ma and 17 ± 5° since 0.8 Ma. The age of the second phase was based on the results obtained from the youngest investigated deposits, i.e. the Ladiko-Tsampika Formation, then considered to have been deposited between 1.1 and 0.8 Ma. Based on the new age constraints on the Ladiko-Tsampika Formation (this study), this second phase occurred more recently, after *c.* 0.14 Ma (Fig. 11), suggesting that the second phase of rotation may have occurred at considerably higher rates than previously estimated.

Quaternary tectonics of Rhodes in the eastern Aegean arc

The plate boundary at the Hellenic trench is highly curved and to the east this peculiar geometry leads to the highly oblique subduction of the African plate below the Aegean plate (Fig. 1). This eastern part of the trench is thus characterized by a transpressive strain pattern rather than regular dip-slip thrusts (McKenzie 1978; Le Pichon & Angelier 1981; Mascle *et al*. 1986). In such tectonic contexts, crustal-scale strike-slip faults delineate independent micro-blocks in terms of strain pattern, vertical motion and bulk deformation (Jarrard 1986). Three blocks can be identified along the eastern Hellenic forearc: Rhodes, Karpathos and Crete (Mascle *et al*. 1986). Karpathos Island was uplifted at a mean rate of 0.27–0.49 mm a^{-1} between 1.730–1.617 Ma (early Zone CNPL8) and 0.26 Ma (Zone CNPL11) based on palaeobathymetric data from presently emerged deep sea coral boundstones (Fig. 11) (Moissette *et al*. 2017). The island rotated 18 ± 12° anticlockwise after *c.* 1.8 Ma (Duermeijer *et al*. 2000). In Crete, inverse modelling of longitudinal river profiles indicates that Crete emerged in the 4–2 Ma interval with uplift rates of *c.* 0.1–0.5 mm a^{-1}; central and eastern Crete was then uplifted at rates of 1–1.2 mm a^{-1} from 1 Ma (Roberts *et al*. 2013) and eastern Crete at a mean rate of 0.5 mm a^{-1} (Strobl *et al*. 2014) (Fig. 11). Counterclockwise rotations of varying amounts were identified, but they are poorly dated after the early Messinian and are presumably significant rotations of individual blocks (Duermeijer *et al*. 1998, 2000).

In comparison with other islands of the central–eastern Hellenic forearc that display uplift (Fig. 11), we show that since 2 Ma Rhodes underwent a unique history of vertical motion of tectonic origin. We show that the eastern coast of Rhodes has experienced two major uplift episodes since the late Gelasian, between 800 and 400 ka and since 33 ka. These two episodes were punctuated by phases of subsidence between 2 and 0.8 Ma and between 0.265 and 0.14 Ma. In Rhodes, uplift and subsidence rates were rather high at 0.32–0.5 to *c.* 2–2.4(?) mm a^{-1}, in the range classically observed in forearc settings (0.5–1.5 to 2 mm a^{-1}; e.g. Henry *et al*. 2014; Pedoja *et al*. 2014). Vertical motions were related to alternating eastward tilting and westward back-tilting around a NNE–SSW-trending horizontal axis (Hanken *et al*. 1996; van Hinsbergen *et al*. 2007) (Fig. 3). The first drowning phase is characterized by a southeastward tilt that could be controlled by NE–SW-trending faults. Differential block tilting inside Rhodes is suspected and needs further investigation. The second episode of uplift is coeval with a large anticlockwise rotation that occurred after 0.33 Ma. We attribute the counterclockwise rotations, together with the uplift and drowning related to rolling of the island, to reflect the progressive accommodation of oblique strain along the transpressive plate boundary in a partitioned way. During oblique subduction, strain is partitioned along strike-slip faults accommodating the motion parallel to the trench and thrust faults accommodating the motion perpendicular to the trench.

In particular, uplift and coeval counterclockwise rotation are here thought to reflect thrusting and shearing along a positive flower structure belonging to the large strike-slip fault. Indeed, the NW-dipping thrusts imaged below the Rhodes Basin could be part of a flower structure (e.g. Woodside *et al*. 2000). Rolling of the island, responsible for the uplift and drowning episodes, may be related to far-field stresses and strain related to thickening of the crust or to the activation of the Rhodes thrust with pure dip-slip kinematics (Kontogianni *et al*. 2002; Hall *et al*. 2014). These two mechanisms would affect Rhodes without significant rotation around a vertical axis, but would be responsible for vertical motion.

Conclusions

The re-examination of numerous exposures of the eastern coast of Rhodes and new dating has resulted in a refined sedimentary model for the time interval since 2 Ma. The coastal basins comprise four synthems (main transgressive–regressive sedimentary cycles) separated by emersion surfaces now considered to be of regional extent, from bottom to top.

(1) The Rhodes Synthem is now restricted to the Kolymbia, Lindos Bay and Cape Arkhangelos formations. The basal part of the synthem deposited from *c.* 2 Ma. The uppermost part of the Cape Arkhangelos Formation is now proved to have deposited between 560 and 458 ka. The synthem is topped by an erosional surface of tectonic origin.
(2) The new Afandou Synthem, which consists of the Ladiko-Tsampika Formation, deposited during the interval 265–114 ka (MIS 8 to MIS 6). The top of the deposits is

underlain by an erosional surface responsible for the formation of the Windmill Bay Formation (boulder bed), previously assigned to the succeeding synthem. The erosional surface is assigned to the MIS 6 low sea-level.

(3) The Lindos-Acropolis Synthem, which is restricted to the Gialos and the Kleopulu formations, deposited between 140 and 50 ka (MIS5e to MIS 4). The synthem is topped by an erosional surface assigned to the MIS 4 low sea-level.

(4) The new Malona Synthem, which consists of the Agathi and Plimiri Formations, deposited between 33 and 17 ka (MIS 3 and MIS 2). The synthem is topped by an erosional surface assigned to the MIS 2 low sea-level.

Between *c.* 2 and *c.* 1 Ma (the Kolymbia and Lindos Bay formations), differential subsidence occurred due to the southeastward tilting of the island, with rates in the range 0.32–0.5 to 2.4 mm a^{-1}. Between *c.* 800 and 400 ka, the eastern part of Rhodes was uplifted as a result of back-tilting with a mean rate of 1.3 mm a^{-1}. Between 265 and 114 ka, a second phase of subsidence occurred with a mean rate of 1.2 mm a^{-1}. From 33 ka eastern Rhodes underwent a second uplift phase with rates ranging between 1.4 and 3.9 mm a^{-1}, coeval with a $17 \pm 9°$ anticlockwise rotation. Such an evolution is unique in the eastern Hellenic forearc. It is interpreted as reflecting the individualization of Rhodes as an independent tectonic block since 2 Ma. We interpret the observed strain pattern and uplift/subsidence history to reflect strain partitioning during the increasing curvature of the forearc.

Acknowledgements We thank Doriane Delmas and Christophe Nevado (University of Montpellier) for the preparation of thin sections. We are grateful to Vasileios Karakitsios and Jürgen Titschack for their constructive reviews of an earlier version of the manuscript.

Funding This work was funded by the National Research programmes Tellus-SYSTER (JJC) and Tellus-INTERRVIE (FQ) of CNRS-INSU.

Scientific editing by Philip Hughes

Correction Notice: An author's name has been updated following a submission error.

References

Aksu, A.E., Hiscott, R.N., Kostylev, V.E. & Yaltırak, C. 2018. Organized patches of bioherm growth where the Strait of Dardanelles enters the Marmara Sea, Turkey. *Palaeogeography, Palaeoclimatology, Palaeoecology*, **490**, 325–346.

Angelier, J., Lybéris, N., Le Pichon, X., Barrier, E. & Huchon, P. 1982. The tectonic development of the Hellenic Arc and the Sea of Crete: a synthesis. *Tectonophysics*, **86**, 159–196.

Backman, J., Raffi, I., Rio, D., Fornaciari, E. & Pälike, H. 2012. Biozonation and biochronology of Miocene through Pleistocene calcareous nannofossils from low and middle latitudes. *Newsletters on Stratigraphy*, **45**, 221–244.

Ballesteros, E. 2006. Mediterranean coralligenous assemblages: a synthesis of present knowledge. *Oceanography and Marine Biology: An Annual Review*, **44**, 123–195.

Baumann, K.-H. & Freitag, T. 2004. Pleistocene fluctuations in the northern Benguela Current system as revealed by coccolith assemblages. *Marine Micropalaeontology*, **52**, 195–215.

Benda, L., Meulenkamp, J.E. & van de Weerd, A. 1977. Biostratigraphic correlations in the Eastern Mediterranean Neogene. 3. Correlation between mammal, sporomorph and marine microfossil assemblages from the Upper Cenozoic of Rhodes, Greece. *Newsletters on Stratigraphy*, **6**, 117–130.

Bollmann, J., Baumann, K.-H. & Thierstein, H.R. 1998. Global dominance of *Gephyrocapsa* coccoliths in the late Pleistocene: selective dissolution, evolution, or global environmental change? *Paleoceanography and Paleoclimatology*, **13**, 517–529.

Bonneau, M. 1984. Correlation of the Hellenide nappes in the south-east Aegean and their tectonic reconstruction. *In*: Dixon, J.E. & Robertson, A.H.F. (eds) *The Geological Evolution of the Eastern Mediterranean*. Geological Society, London, Special Publications, **17**, 517–527, https://doi.org/10.1144/GSL.SP.1984.017.01.38

Boyd, A. 2009. Relict conifers from the mid-Pleistocene of Rhodes, Greece. *Historical Biology*, **21**, 1–15.

Broekman, J.A. 1974. Sedimentation and palaeoecology of Pliocene lagoonal-shallow marine deposits on the Island of Rhodes (Greece). *Utrecht Micropalaeontological Bulletins*, **8**, 1–142.

Brun, J.P. & Faccenna, C. 2008. Exhumation of high-pressure rocks driven by slab rollback. *Earth and Planetary Science Letters*, **272**, 1–7.

Brun, J.P., Faccenna, C., Gueydan, F., Sokoutis, D., Philippon, M., Kydonakis, K. & Gorini, C. 2016. The two-stage Aegean extension, from localized to distributed, a result of slab rollback acceleration. *Canadian Journal of Earth Sciences*, **53**, 1142–1157.

Carminati, E., Giunchi, C., Argnani, A., Sabadini, R. & Fernandez, M. 1999. Plio-Quaternary vertical motion of the Northern Apennines: insights from dynamic modelling. *Tectonics*, **18**, 703–718.

Cita, M.B., Gibbard, P.L., Head, M.J. & and the ICS Subcommission on Quaternary Stratigraphy 2012. Formal ratification of the GSSP for the base of the Calabrian Stage (second stage of the Pleistocene Series, Quaternary System). *Episodes*, **35**, 388–397.

Clift, P. & Vannucchi, P. 2004. Controls on tectonic accretion versus erosion in subduction zones: implications for the origin and recycling of the continental crust. *Reviews of Geophysics*, **42**, 1–31, https://doi.org/10.1029/2003RG000127

Cloething, S. & Burov, E. 2011. Lithospheric folding and sedimentary basin evolution: a review and analysis of formation mechanisms. *Basin Research*, **23**, 257–290.

Cloething, S., Bada, G., Matenco, L., Lankreijer, A., Horváth, F. & Dinu, C. 2006. Modes of basin (de)formation, lithospheric strength and vertical motions in the Pannonian–Carpathian system: inferences from thermo-mechanical modelling. *In*: Gee, D.G. & Stephenson, R.A. (eds) *European Lithosphere Dynamics*. Geological Society, London, Memoirs, **32**, 207–221, https://doi.org/10.1144/GSL.MEM.2006.032.01.12

Cornée, J.J., Moissette, P. *et al.* 2006*a*. Tectonic and climatic controls on coastal sedimentation: the Late Pliocene–Middle Pleistocene of northeastern Rhodes, Greece. *Sedimentary Geology*, **187**, 159–181.

Cornée, J.J., Münch, P. *et al.* 2006*b*. Timing of Late Pliocene to Middle Pleistocene tectonic events in Rhodes (Greece) inferred from magneto-biostratigraphy and $^{40}Ar/^{39}Ar$ dating of a volcaniclastic layer. *Earth and Planetary Science Letters*, **250**, 281–291.

Duermeijer, C.E., Krijgsman, W., Langereis, C.G. & Ten Veen, J.H. 1998. Post-early Messinian counterclockwise rotations on Crete: implications for Late Miocene to Recent kinematics of the southern Hellenic arc. *Tectonophysics*, **298**, 177–189.

Duermeijer, C.E., Nyst, M., Meijer, P.T., Langereis, C.G. & Spakman, W. 2000. Neogene evolution of the Aegean Arc: palaeomagnetic and geodetic evidence for a rapid and young rotation phase. *Earth and Planetary Science Letters*, **176**, 509–525.

Fietzke, J., Liebetrau, V., Eisenhauer, A. & Dullo, C. 2005. Determination of uranium isotope ratios by multi-static MIC-ICP-MS: method and implementation for precise U- and Th-series isotope measurements. *Journal of Analytical Atomic Spectrometry*, **20**, 395–401.

Flores, J.-A., Gersonde, R. & Sierro, F.J. 1999. Pleistocene fluctuations in the Agulhas Current Retroflection based on the calcareous plankton record. *Marine Micropalaeontology*, **37**, 1–22.

Frydas, D. 1994. Die Pliozän/Pleistozän-Grenze auf der Insel Rhodes (Griechenland). *Münstersche Forschungen zur Geologie und Paläontologie*, **76**, 331–344.

Gautier, P., Brun, J.-P., Moriceau, R., Sokoutis, D., Martinod, J. & Jolivet, L. 1999. Timing, kinematics and cause of the Aegean extension: a scenario based on comparison with simple analogue experiments. *Tectonophysics*, **315**, 31–72.

Gradstein, F.M., Ogg, J.G., Schmitz, M.D. & Ogg, G.M. (eds) 2012. *The Geological Time Scale*. Elsevier, Amsterdam.

Hall, J., Aksu, A.E., Yaltırak, C. & Winsor, J.D. 2009. Structural architecture of the Rhodes Basin: a deep depocentre that evolved since the Pliocene at the junction of Hellenic and Cyprus Arcs, eastern Mediterranean. *Marine Geology*, **258**, 1–23.

Hall, J., Aksu, A.E., Elitez, I., Yaltırak, C. & Çifçi, G. 2014. The Fethiye–Burdur Fault Zone: a component of upper plate extension of the subduction transform edge propagator fault linking Hellenic and Cyprus Arcs, Eastern Mediterranean. *Tectonophysics*, **635**, 80–99. https://doi.org/10.1016/j.tecto.2014.05.002

Hanken, N.-M., Bromley, R.G. & Miller, J. 1996. Plio-Pleistocene sedimentation in coastal grabens, north-east Rhodes, Greece. *Geological Journal*, **31**, 271–296.

Hansen, K.S. 1999. Development of a prograding carbonate wedge during sea level fall: Lower Pleistocene of Rhodes, Greece. *Sedimentology*, **46**, 559–576.

Henry, H., Regard, V., Pedoja, K., Husson, L., Martinod, J., Witt, C. & Heuret, A. 2014. Upper Pleistocene uplifted shorelines as tracers of (local rather than global) subduction dynamics. *Journal of Geodynamics*, **78**, 8–20.

Isacks, B.L. 1988. Uplift of the central Andean plateau and bending of the Bolivian orocline. *Journal of Geophysical Research*, **93**, 3211–3231.

Jarrard, R.D. 1986. Terrane motion by strike-slip faulting of forearc slivers. *Geology*, **14**, 780–783.

Joannin, S., Cornée, J.J. *et al.* 2007. Changes in vegetation and marine environments in the eastern Mediterranean (Rhodes Island, Greece) during the Early and Middle Pleistocene. *Journal of the Geological Society, London*, **164**, 1119–1131, https://doi.org/10.1144/0016-76492006-136

Jolivet, L. & Brun, J.P. 2010. Cenozoic geodynamic evolution of the Aegean. *International Journal of Earth Sciences*, **99**, 109–138.

Jolivet, L., Faccenna, C. *et al.* 2013. Aegean tectonics: strain localisation, slab tearing and trench retreat. *Tectonophysics*, **597–598**, 1–33.

Katili, J.A. 1970. Large transcurrent faults in Southeast Asia with special reference to Indonesia. *Geologische Rundschau*, **59**, 581–600.

Kawagata, S., Hayward, B.W., Grenfell, H.R. & Sabaa, A. 2005. Mid-Pleistocene extinction of deep-sea foraminifera in the North Atlantic Gateway (ODP sites

980 and 982). *Palaeogeography, Palaeoclimatology, Palaeoecology*, **221**, 267–291.
Kaymakcı, N., Langereis, C., Özkaptan, M., Özacar, A.A., Gülyüz, E., Uzel, B. & Sözbilir, H. 2018. Paleomagnetic evidence for upper plate response to a STEP fault, SWAnatolia. *Earth and Planetary Science Letters*, **498**, 101–115.
Keraudren, B. 1970. Les formations quaternaires marines de la Grèce. *Bulletin du Musée d'Anthropologie préhistorique de Monaco*, **6**, 5–153.
Kontogianni, V.A., Tsoulos, N. & Stiros, S.C. 2002. Coastal uplift, earthquakes and active faulting of Rhodes Island (Aegean Arc): modeling based on geodetic inversion. *Marine Geology*, **186**, 299–317.
Kovacs, E. & Spjeldnaes, N. 1999. Pliocene–Pleistocene stratigraphy of Rhodes, Greece. *Newsletters on Stratigraphy*, **37**, 191–208.
Lallemand, S. 1999. *La subduction océanique*. Editions Scientifiques/Gordon and Breach, London, UK.
Lekkas, E., Papanikolaou, D. & Sakellariou, D. 2000. *Neotectonic Map of Greece, Rhodes Sheet 1:100,000*. Tectonic Committee of the Geological Society of Greece, Athens.
Le Pichon, X. & Angelier, J. 1981. The Aegean Sea. *Philosophical Transactions of the Royal Society of London, Series A*, **300**, 357–372.
Linse, U. 2016. The marine Plio-Pleistocene of Rhodes, Greece: a Mediterranean climate archive. *Documenta Naturae*, **SB76**, 1–143.
Lisiecki, L.E. & Raymo, M.E. 2005. A Pliocene–Pleistocene stack of 57 globally distributed benthic $\delta^{18}O$ records. *Palaeoceanography*, **20**, PA1003, https://doi.org/10.1029/2004PA001071
López-Otálvaro, G.-E., Flores, J.-A., Sierro, F.J. & Cacho, I. 2008. Variations in coccolithophorid production in the Eastern Equatorial Pacific at ODP Site 1240 over the last seven glacial–interglacial cycles. *Marine Micropalaeontology*, **69**, 52–69.
Lourens, L.J., Hilgen, F.J. & Raffi, I. (eds) 1998. Base of large Gephyrocapsa and astronomical calibration of early Pleistocene sapropels in site 967 and Hole 969D: solving the chronology of the Vrica section (Calabria, Italy). *Proceedings of the Ocean Drilling Program, Scientific Results*, **160**. Ocean Drilling Program, College Station, TX, 191–197.
Lourens, L.J., Hilgen, F.J., Laskar, J., Shackleton, N.J. & Wilson, D.S. 2004. The Neogene Period. *In*: Gradstein, F.M., Ogg, J.G. & Smith, A.G. (eds) *A Geologic Time Scale 2004*. Cambridge University Press, Cambridge, 409–440.
Løvlie, R., Støle, G. & Spjeldnaes, N. 1989. Magnetic polarity stratigraphy of Pliocene–Pleistocene marine sediments from Rhodes, eastern Mediterranean. *Physics of the Earth and Planetary Interiors*, **54**, 340–352.
Mackay, L.M., Turner, J., Jones, S.M. & White, N.J. 2005. Cenozoic vertical motions in the Moray Firth Basin associated with initiation of the Iceland Plume. *Tectonics*, **24**, TC5004, https://doi.org/10.1029/2004TC001683
Maier, E. & Tistschack, J. 2010. *Spondylus gaederopus*: a new Mediterranean climate archive — based on-high resolution oxygen and carbon isotope analyses. *Palaeogeography, Palaeoclimatology, Palaeoecology*, **291**, 228–238.
Mascle, J., Le Cleac'h, A. & Jongsma, D. 1986. The eastern Hellenic margin from Crete to Rhodes: example of progressive collision. *Marine Geology*, **73**, 145–168.
McCaffrey, R. 2009. The tectonic framework of the Sumatran subduction zone. *Annual Review of Earth and Planetary Sciences*, **37**, 345–366.
McKenzie, D. 1978. Some remarks on the development of sedimentary basins. *Earth and Planetary Science Letters*, **40**, 25–32.
Merzeraud, G. 2017. *Sédimentologie*. DeBoeck-Supérieur, Paris.
Meulenkamp, J.E., De Mulder, E.F.J. & Van De Weerd, A. 1972. Sedimentary history and palaeogeography of the Late Cenozoic of the Island of Rhodes. *Zeitschrift der Deutschen Geologischen Gesellschaft*, **123**, 541–553.
Meulenkamp, J.E., van der Zwaan, G.J. & van Wamel, W.A. 1994. On late Miocene to Recent vertical motions in the Cretan segment of the Hellenic arc. *Tectonophysics*, **234**, 53–72.
Milker, Y., Weinkauf, M.F.G., Titschack, J., Freiwald, A., Krüger, S., Jorissen, F.J. & Schmiedl, G. 2017. Testing the applicability of a benthic foraminiferal-based transfer function for the reconstruction of palaeowater depth changes in Rhodes (Greece) during the early Pleistocene. *PLoS One*, **12**, e0188447, https://doi.org/10.1371/journal.pone.0188447
Moissette, P. & Spjeldnaes, N. 1995. Plio-Pleistocene deep-water bryozoans from Rhodes, Greece. *Palaeontology*, **38**, 771–799.
Moissette, P., Koskeridou, E., Cornée, J.J., Guillocheau, F. & Lécuyer, C. 2007. Spectacular preservation of seagrasses and seagrass-associated communities from the Pliocene of Rhodes, Greece. *Palaios*, **22**, 200–211.
Moissette, P., Cornée, J.J. & Koskeridou, E. 2010. Pleistocene rolling stones or large bryozoan nodules in a mixed siliciclastic-carbonate environment (Rhodes, Greece). *Palaios*, **25**, 24–39.
Moissette, P., Koskeridou, E., Cornée, J.J. & André, J.P. 2013. Fossil assemblages associated with submerged beachrock beds as indicators of environmental changes in terrigenous sediments: examples from the Gelasian (Early Pleistocene) of Rhodes, Greece. *Palaeogeography, Palaeoclimatology, Palaeoecology*, **369**, 14–27.
Moissette, P., Koskeridou, E., Drinia, H. & Cornée, J.J. 2016. Facies associations in warm-temperate siliciclastic deposits: insights from early Pleistocene eastern Mediterranean (Rhodes, Greece). *Geological Magazine*, **153**, 61–83.
Moissette, P., Cornée, J.J., Quillévéré, F., Zibrowius, H., Koskeridou, E. & López-Otálvaro, G.E. 2017. Pleistocene (Calabrian) deep-water corals and associated biodiversity in the eastern Mediterranean (Karpathos Island, Greece). *Journal of Quaternary Science*, **32**, 923–933.
Morris, A. & Robertson, A.H.F. 1993. Miocene remagnetisation of carbonate platform and Antalya Complex units within the Isparta angle, SW Turkey. *Tectonophysics*, **220**, 243–266.
Mutti, E., Orombelli, G. & Pozzi, R. 1970. Geological map of Rhodes Island (Greece) and geological studies on the Dodecanese Islands (Aegean Sea). IX. Geological map of the island of Rhodes (Greece); explanatory notes. *Annales Géologiques des Pays Helléniques*, **22**, 79–226.
Nelson, C.S., Freiwald, A., Titschack, J. & List, S. 2001. *Lithostratigraphy and Sequence Architecture of Temperate Mixed Siliciclastic-Carbonate Facies in a New Plio-Pleistocene Section at Plimiri, Rhodes Island (Greece)*. Occasional Reports, **25**. Department of Earth Sciences, University of Waikato, Hamilton.
Nielsen, J.K., Hanken, N.-M., Nielsen, J.K. & Hansen, K.S. 2006. Biostratigraphy and palaeoecology of the marine Pleistocene of Rhodes, Greece: Scleractinia, Serpulidae, Mollusca and Brachiopoda. *Bulletin of Geosciences*, **81**, 173–196.
Pedoja, K., Husson, L., *et al.* 2014. Coastal staircase sequences reflecting sea-level oscillations and tectonic uplift during the Quaternary and Neogene. *Earth-Science Reviews*, **132**, 13–38, https://doi.org/10.1016/j.earscirev.2014.01.007
Philippon, M., Brun, J.-P., Gueydan, F. & Sokoutis, D. 2014. The interaction between Aegean back-arc extension and Anatolia escape since Middle Miocene. *Tectonophysics*, **631**, 176–188.
Pirazzoli, P.A., Montaggioni, L.F., Saliege, J.F., Segonzac, G., Thommeret, Y. & Vergnaud-Grazzini, C. 1989. Crustal block movements from Holocene shorelines: Rhodes Island (Greece). *Tectonophysics*, **170**, 89–114.
Quillévéré, F., Cornée, J.J., *et al.* 2016. Chronostratigraphy of uplifted Quaternary hemipelagic deposits from the Dodecanese island of Rhodes (Greece). *Quaternary Research*, **86**, 79–94.
Raffi, I., Backman, J., Fornaciari, E., Pälike, H., Rio, D., Lourens, L. & Hilgen, F. 2006. A review of calcareous nannofossil astrobiochronology encompassing the past 25 million years. *Quaternary Science Reviews*, **25**, 3113–3137.
Rasmussen, T.L. & Thomsen, E. 2005. Foraminifera and palaeoenvironment of the Plio-Pleistocene Kallithea Bay section, Rhodes, Greece: evidence for cyclic sedimentation and shallow-water sapropels. *Cushman Foundation for Foraminiferal Research, Special Publications*, **39**, 15–51.
Rasmussen, T.L., Hastrup, A. & Thomsen, E. 2005. Lagoon to deep-water foraminifera and ostracods from the Plio-Pleistocene Kallithea bay section, Rhodes, Greece. *Cushman Foundation for Foraminiferal Research*, Special Publications, **39**, 292–293.
Roberts, G.G., White, N.J. & Shaw, B. 2013. An uplift history of Crete, Greece, from inverse modeling of longitudinal river profiles. *Geomorphology*, **198**, 177–188.
Rohling, E.J., Hibbert, F.D., *et al.* 2017. Differences between the last two glacial maxima and implications for ice-sheet, $\delta^{18}O$, and sea-level reconstructions. *Quaternary Science Reviews*, **176**, 1–28, https://doi.org/10.1016/j.quascirev.2017.09.009
Saillard, M., Audin, L., *et al.* 2017. From the seismic cycle to long-term deformation: linking seismic coupling and Quaternary coastal geomorphology along the Andean megathrust. *Tectonics*, **36**, 241–256, https://doi.org/10.1002/2016TC004156
Sakellariou, D., Mascle, J. & Lykousis, V. 2013. Strike slip tectonics and transtensional deformation in the Aegean region and the Hellenic arc: Preliminary results. *Bulletin of the Geological Society of Greece*, **47**, 647–656, https://doi.org/10.12681/bgsg.11098
Salvador, A. 1994. *International Stratigraphic Guide – A Guide to Stratigraphic Classification, Terminology, and Procedure*. International Union of Geological Sciences/Geological Society of America, Washington, DC.
Schlaphorst, D., Kendall, J.M., *et al.* 2016. Water, oceanic fracture zones and the lubrication of subducting plate boundaries—insights from seismicity. *Geophysical Journal International*, **204**, 1405–1420. https://doi.org/10.1093/gji/ggv509
Shemenda, A.I. 1994. *Subduction. Insights from Physical Modeling*. Kluwer Academic, Dordrecht.
Sissingh, W. 1972. Late Cenozoic Ostracoda of the South Aegean Island Arc. *Utrecht Micropalaeontological Bulletins*, **6**, 1–187.
Steinthorsdottir, M. & Hakansson, E. 2017. Endo- and epilithic faunal succession in a Pliocene-Pleistocene cave on Rhodes, Greece: record of a transgression. *Palaeontology*, **60**, 663–681, https://doi.org/10.1111/pala.12312
Steinthorsdottir, M., Lidgard, S. & Hakansson, E. 2006. Fossils, sediments, tectonics. Reconstructing palaeoenvironments in a Pliocene–Pleistocene Mediterranean microbasin. *Facies*, **52**, 361–380.
Strobl, M., Hetzel, R., Fassoulas, C. & Kubik, P.W. 2014. A long-term rock uplift rate for eastern Crete and geodynamic implications for the Hellenic subduction zone. *Journal of Geodynamics*, **78**, 21–31.
ten Veen, J.H. 2004. Extension of Hellenic forearc shear zones in SW Turkey: the Pliocene–Quaternary deformation of the Eşen Çay Basin. *Journal of Geodynamics*, **37**, 181–204.
ten Veen, J.H., Boulton, S.J. & Alçiçek, M.C. 2009. From palaeotectonics to neotectonics in the Neotethys realm: the importance of kinematic decoupling and inherited structural grain in SW Anatolia (Turkey). *Tectonophysics*, **473**, 261–281.
Thierstein, H.R., Geitzenauer, K.R., Molfino, B. & Shackleton, N.J. 1977. Global synchroneity of late Quaternary coccolith datum levels: validation by oxygen isotopes. *Geology*, **5**, 400–404.

Thomsen, E., Rasmussen, T.L. & Hastrup, A. 2001. Calcareous nannofossil, ostracode and foraminifera biostratigraphy of Plio-Pleistocene deposits, Rhodes (Greece), with a correlation to the Vrica section (Italy). *Journal of Micropalaeontology*, **20**, 143–154, https://doi.org/10.1144/jm.20.2.143

Thomsen, E., Knudsen, J. & Koskeridou, E. 2009. Fossil panopeans (Bivalvia, Hiatellidae) from Rhodes, Greece. *Steenstrupia*, **30**, 163–176.

Titschack, J., Bromley, R.G. & Freiwald, A. 2005. Plio-Pleistocene cliff-bound, wedge-shaped, warm-temperate carbonate deposits from Rhodes (Greece): sedimentology and facies. *Sedimentary Geology*, **180**, 29–56.

Titschack, J., Nelson, C.S., Beck, T., Freiwald, A. & Radtke, U. 2008. Sedimentary evolution of a Late Pleistocene temperate red algal reef (Coralligène) on Rhodes, Greece: correlation with global sea-level fluctuations. *Sedimentology*, **55**, 1747–1776.

Titschack, J., Joseph, N., Fietzke, J., Freiwald, A. & Bromley, R.G. 2013. Record of a tectonically-controlled regression captured by changes in carbonate skeletal associations on a structured island shelf (mid-Pleistocene, Rhodes, Greece). *Sedimentary Geology*, **283**, 15–33.

Tur, H., Yaltırak, C., Elitez, İ & Sarıkavak, K.T. 2015. Pliocene–Quaternary tectonic evolution of the Gulf of Gökova, southwest Turkey. *Tectonophysics*, **638**, 158–176.

van der Meulen, M.J., Kouwenhoven, T.J., van der Zwaan, G.J., Meulenkamp, J.E. & Wortel, M.J.R. 1999. Late Miocene uplift in the Romagnan Apennines and the detachment of subducted lithosphere. *Tectonophysics*, **315**, 319–335.

van Hinsbergen, D. 2004. *The evolving anatomy of a collapsing orogen*. Geologica Ultraiectina, Mededelingen van de faculteit Geowetenschappen Universiteit Utrecht, **243**.

van Hinsbergen, D.J.J. & Schmid, S.M. 2012. Map view restoration of Aegean–West Anatolian accretion and extension since the Eocene. *Tectonics*, **31**, TC5005, https://doi.org/10.1029/2012TC003132

van Hinsbergen, D.J.J., Hafkenscheid, E., Spakman, W., Meulenkamp, J.E. & Wortel, R. 2005*a*. Nappe stacking resulting from subduction of oceanic and continental lithosphere below Greece. *Geology*, **33**, 325–328.

van Hinsbergen, D.J.J., Langereis, C.G. & Meulenkamp, J.E. 2005*b*. Revision of the timing, magnitude and distribution of Neogene rotations in the western Aegean region. *Tectonophysics*, **396**, 1–34.

van Hinsbergen, D.J.J., Krijgsman, W., Langereis, C.G., Cornée, J.J., Duermeijer, C.E. & van Vugt, N. 2007. Discrete Plio-Pleistocene phases of tilting and counterclockwise rotation in the southeastern Aegean arc (Rhodes, Greece): early Pliocene formation of the south Aegean left-lateral strike-slip system. *Journal of the Geological Society, London*, **164**, 1133–1144, https://doi.org/10.1144/0016-76492006-061

Vergés, J., Marzo, M., Santaeulària, T., Serra-Kiel, J., Burbank, D.W., Muñoz, J.A. & Giménez-Montsant, J. 1998. Quantified vertical motions and tectonic evolution of the SE Pyrenean foreland basin. *In*: Mascle, A., Puigdefabregas, C., Luterbacher, H.R. & Fernandez, M. (eds) *Cenozoic Foreland Basins of Western Europe*. Geological Society, London, Special Publications, **134**, 107–134, https://doi.org/10.1144/GSL.SP.1998.134.01.06

von Huene, R. & Ranero, C.R. 2003. Subduction erosion and basal friction along the sediment-starved convergent margin off Antofagasta *Chile. Journal of Geophysical Research: Solid Earth*, **108**, https://doi.org/10.1029/2001JB001569

Wallace, L.M., McCaffrey, R., Beavan, J. & Ellis, S. 2005. Rapid microplate rotations and backarc rifting at the transition between collision and subduction. *Geology*, **33**, 857–860, https://doi.org/10.1130/G21834.1

Wallace, L.M., Ellis, S. & Mann, P. 2008. Tectonic block rotation, arc curvature, and back-arc rifting: insights into these processes in the Mediterranean and the western Pacific. *IOP Conference Series: Earth and Environmental Sciences*, **2**, 012010, https://doi.org/10.1088/1755-1307/2/1/012010

Weinholz, P. & Lutze, G.F. 1989. The *Stilostomella* extinction. *In*: Baldauf, J., Heath, G.G., Ruddiman, W.F. & Sarnthein, M. (eds) *Proceedings of the Ocean Drilling Program, Scientific Results*, **108**. Ocean Drilling Program, College Station, TX, 113–117.

Woodside, J., Mascle, J., Huguen, C. & Volkonskaia, A. 2000. The Rhodes Basin, a post-Miocene tectonic trough. *Marine Geology*, **165**, 1–12.